

CATIONIC RUTHENIUM CATALYSTS FOR OLEFIN HYDROVINYLATION

A Thesis

by

RICHARD P. SANCHEZ, JR.

Submitted to the Office of Graduate Studies of
Texas A&M University
in partial fulfillment of the requirements for the degree of

MASTER OF SCIENCE

August 2009

Major Subject: Chemistry

CATIONIC RUTHENIUM CATALYSTS FOR OLEFIN HYDROVINYLATION

A Thesis

by

RICHARD P. SANCHEZ, JR.

Submitted to the Office of Graduate Studies of
Texas A&M University
in partial fulfillment of the requirements for the degree of

MASTER OF SCIENCE

Approved by:

Chair of Committee,	Brian T. Connell
Committee Members,	Kevin Burgess
	Daniel Romo
	Rayford G. Anthony
Head of Department,	David H. Russell

August 2009

Major Subject: Chemistry

ABSTRACT

Cationic Ruthenium Catalysts for Olefin Hydrovinylation.

(August 2009)

Richard P. Sanchez, Jr., B.S., M.S., Texas A&M University-Kingsville

Chair of Advisory Committee: Dr. Brian T. Connell

Stereoselective carbon-carbon bond formation is one of the most important types of bond construction in organic chemistry. A mild and acid free catalyst system for the hydrovinylation reaction utilizing a cationic, ruthenium center is described. A catalytic amount of $\text{RuHCl}(\text{CO})(\text{PCy}_3)_2$ (**2**) activated with AgOTf or AgSbF_6 at room temperature was found to be an effective catalyst system for the hydrovinylation of vinylarenes and the intramolecular hydrovinylation (IHV) of 1,6-dienes.

Vinylarenes with both electron-donating and electron-withdrawing substituents reacted with ethylene at room temperature to provide the desired 3-arylbutenes in moderate to excellent yield (60-99%) under mild reaction conditions, while the IHV reaction of 1,6 dienes provided greater than 90% of product conversion. We also developed the first hydrovinylation catalyst containing a chelating, bidentate phosphine ligand that provides the desired product.

Our ruthenium-based catalytic system has also proven to give an appealing reactivity profile in favor of the desired arylbutenes without promoting undesirable oligomerization and isomerization.

DEDICATION

This thesis is dedicated to my wife,
Denise Sanchez.

ACKNOWLEDGEMENTS

I would like to thank my chair committee member, Professor Brian T. Connell, for his support throughout my time here in Texas A&M University. Brian, thank you for helping me develop into a better scientist and giving me the freedom to try different ideas when it came to chemistry.

I would also like to extend my thanks to my defense committee, Professor Kevin Burgess, Professor Daniel Romo, and Professor Rayford G. Anthony.

To my colleagues and friends in the Connell Group: Alex Bugarin, Maria Duran Galvan, and Jun Yong Kang, thanks for being around and supportive throughout my time here and the lunches, how can I forget. I can't because I'm always hungry.

Finally, thanks to my family for their encouragement and to my wife for her patience and love.

TABLE OF CONTENTS

	Page
ABSTRACT	iii
DEDICATION.....	iv
ACKNOWLEDGEMENTS.....	v
TABLE OF CONTENTS	vi
LIST OF FIGURES.....	viii
LIST OF TABLES.....	ix
 CHAPTER	
I INTRODUCTION	1
1.1 History of the Hydrovinylation Reaction	1
1.2 Mechanism of the Hydrovinylation Reaction.....	4
1.3 Nickel and Palladium Catalyzed Reactions.....	6
1.4 Ruthenium Catalyzed Reactions.....	11
1.5 Specific Aim.....	13
II INVESTIGATION OF A RUTHENIUM-BASED CATALYST	
SYSTEM FOR THE HYDROVINYLLATION REACTION.....	15
2.1 Initial Study and Application.....	15
2.2 Mode of Deactivation	20
III INTRODUCING CHELATING, BIDENTATE PHOSPHINE	
LIGANDS TO THE RUTHENIUM METAL CENTER	23
3.1 Bidentate Phosphine Ligands	23
3.2 RuHCl(CO)(PPh ₃) for the Hydrovinylation Reaction.....	25
3.3 Synthesis of Modified Ruthenium (II) Hydride Complexes	26
3.4 Chelating, Bidentate Phosphine Borane Ligands	27

CHAPTER	Page
3.5 New Catalyst Featuring Chelating, Bidentate Phosphine Ligands	30
3.6 Commercially Available Phosphine Ligands	33
IV INVESTIGATION OF A RUTHENIUM-BASED CATALYST SYSTEM FOR THE INTRAMOLECULAR HYDROVINYLTATION REACTION	36
4.1 Intramolecular Hydrovinylation Reactions	36
4.2 Plausible Catalytic Desymmetrization IHV Reaction	39
4.3 Natural Product Synthesis	40
V CONCLUSION	42
VI EXPERIMENTAL.....	43
6.1 Experimental Section General Considerations	43
6.2 Typical Reaction Procedure for the Hydrovinylation Reaction	44
6.3 Synthesis of the Hydrovinylation Catalysts.....	47
REFERENCES	50
APPENDIX A: NMR SPECTRA.....	53
APPENDIX B: CRYSTAL STRUCTURE OF (<i>R,R</i>)-1,2-BIS(BORANATO (CYCLO-HEXYL)BENZYLPHOSPHINO)ETHANE.....	69
APPENDIX C: CRYSTAL STRUCTURE OF (<i>R,R</i>)-1,2-BIS(BORANATO (<i>I</i> -PROPYL)BENZYLPHOSPHINO)ETHANE	85
VITA.....	93

LIST OF FIGURES

FIGURE		Page
1	Derivatives of Feringa's Phosphoramidite Ligands	8
2	Possible Bimolecular Decomposition Model in Reaction	22
3	Design of New Pentavalent Ruthenium Hydride Complexes	23
4	Desired New Active Catalysts for the Hydrovinylation Reaction.....	32
5	Commercially Available Ligands	34
6	Natural Products: Aureothin and Avermectin A1a.....	35

LIST OF TABLES

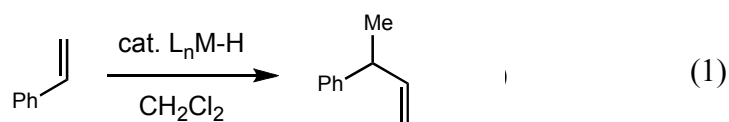
TABLE		Page
1	Hydrovinylation of Vinylarenes Catalyzed by 2 /AgX	17
2	Hydrovinylation of Vinylarenes and Indole Derivatives Catalyzed by 2 /AgX	19
3	Effect of Catalyst Concentration	21
4	Intramolecular Hydrovinylation of 1,6-Dienes Catalyzed by 2 /AgX.....	37

CHAPTER I

INTRODUCTION

1.1 History of the Hydrovinylation Reaction

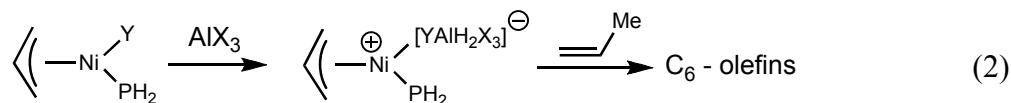
Stereoselective carbon-carbon bond formation is arguably one of the most important transformations in organic chemistry. However, there have been surprisingly few methods developed to construct these bonds directly from prochiral olefins, even though reactions such as these could have a potentially large impact on the chemical and pharmaceutical industry. Metal-catalyzed hydrovinylation, depicted in eq 1 for styrene and ethylene, is the addition of a hydrogen and a vinyl group across an alkene. This has shown to be a useful, regioselective method to generate new carbon-carbon bonds.^{1,2}



An important class of carbon-carbon bond forming reactions is the $[\text{Ni}^+\text{-H}]$ catalyzed oligomerization of olefins. This procedure forms the basis of dimersol^{3,4} technology (eq 2) and the shell higher olefin process (SHOP)⁴ (eq 3). These two processes illustrate the rewards of progressive organometallic research, demonstrating the role of catalyst tuning to achieve highly selective carbon-carbon bond forming reactions. The catalytic dimerization of propene proceeds with such a high rate ($\text{TOF} > 625,000 \text{ [propene] Ni}^{-1} \text{ h}^{-1}$) making this technology one of the best homogeneously catalyzed reactions known (eq 2).*

This thesis follows the style of the *Journal of American Chemical Society*.

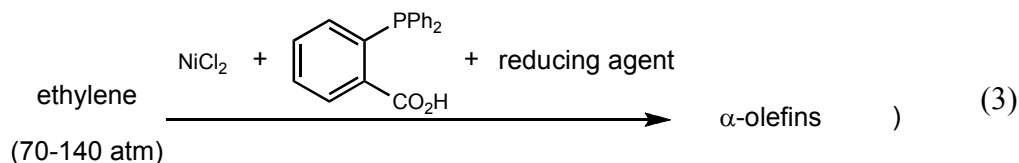
Dimersol technology



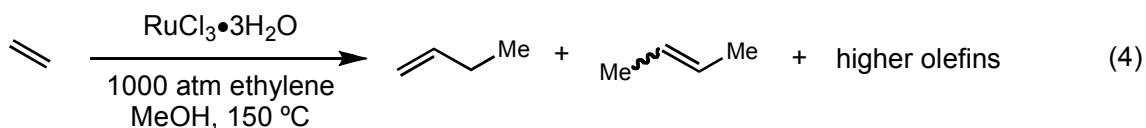
$$\text{TOF} > 625,000 \text{ [propene] Ni}^{-1} \text{ h}^{-1}$$

- Selectivity depends on phosphine and temperature

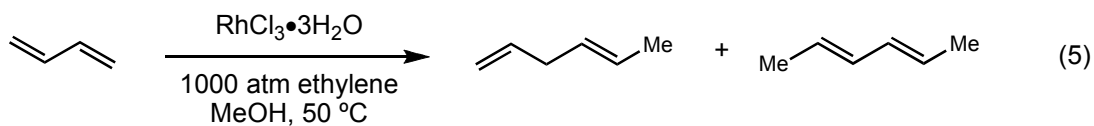
SHOP



In 1965, Alderson, Jenner and Lindsey achieved the first transition-metal catalyzed hydrovinylation of an alkene by using hydrated Rh to affect the codimerization of ethylene.⁵ These reactions took place in an alcoholic media, using high pressure (1000 atm) and heating at 50 °C. A variety of olefins including butadiene and styrene, could also be dimerized. Ruthenium chloride was not an effective catalyst for the dimerization of ethylene. An increase in temperature to 150 °C provided a mixture containing 70% of butenes and 30% of higher olefins presumed to be hexenes and octenes (eq 4).

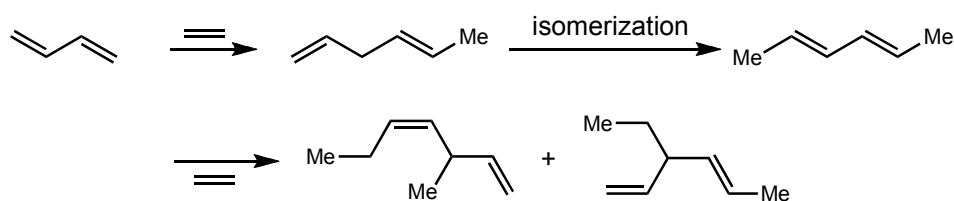


The codimerization of ethylene and butadiene with rhodium chloride catalyst proceeded smoothly to obtain 90% conversion of starting material to obtain a mixture of 1,4- and 2,4-hexadiene (eq 5).

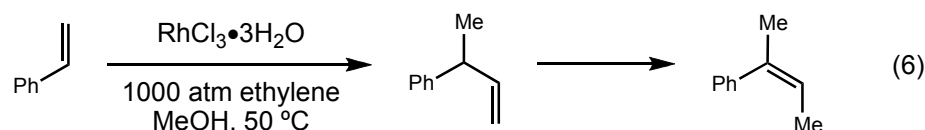


With the use of excess ethylene in the system, C₈-diolefins were formed. This suggested that 1,4-hexadiene was the initial compound formed, but isomerization and further reaction with the excess ethylene provided conjugated C₈-diolefins (Scheme 1).

Scheme 1

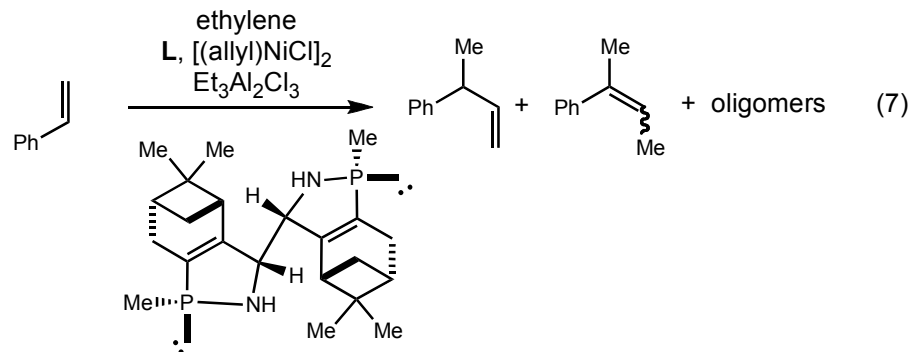


Codimerization of ethylene and styrene was also performed using rhodium chloride delivering 2-phenyl-2-butene (40% yield) using the same reaction conditions aforementioned (eq 6). It was presumed that 3-phenylbutene was first to form followed by isomerization to give the observed product.



Few catalysts had been used in early studies, but typically nickel and palladium catalysts were used due to their higher reactivity. Catalysts that have been used for olefin hydrovinylation are: RhCl₃·3H₂O,⁵ Ni(Ar)(Br)(PR₃)₂-BF₃·OEt₂,^{6,7} PdCl₂-(PhCN)₂,⁸ Pd(OAc)₂/Et₂P(CH₂)₃PEt₂/*p*-toluenesulfonic acid,⁹ PhPd(PPh₃)₂X·H₂O,¹⁰ Co(acac)_x/DPPE/Et_yAl₂Cl_{6-y},¹¹ and RuCl₃/RuCl₄·*n*H₂O,^{5,12} Ni(acac)₂/DPPE/Et_yAl₂Cl_{6-y}.^{11,13}

Among these early studies, Wilke and co-workers demonstrated that asymmetric hydrovinylation of 1,3-cyclooctadiene,¹⁴ norbornene, norbornadiene, styrene (eq 7), and codimerization of propene and 2-butene using a combination of $[(\eta^3\text{-C}_3\text{H}_5)\text{NiCl}]_2$ / $\text{Et}_3\text{Al}_2\text{Cl}_3$ and monoterpene-derived chiral phosphines was possible.¹⁵ In an attempt to broaden the applicability of the hydrovinylation reaction, ensuing effort was aimed at simplifying the phosphine motif and removal of the Lewis acid needed to activate the reaction in Wilke's catalyst system.

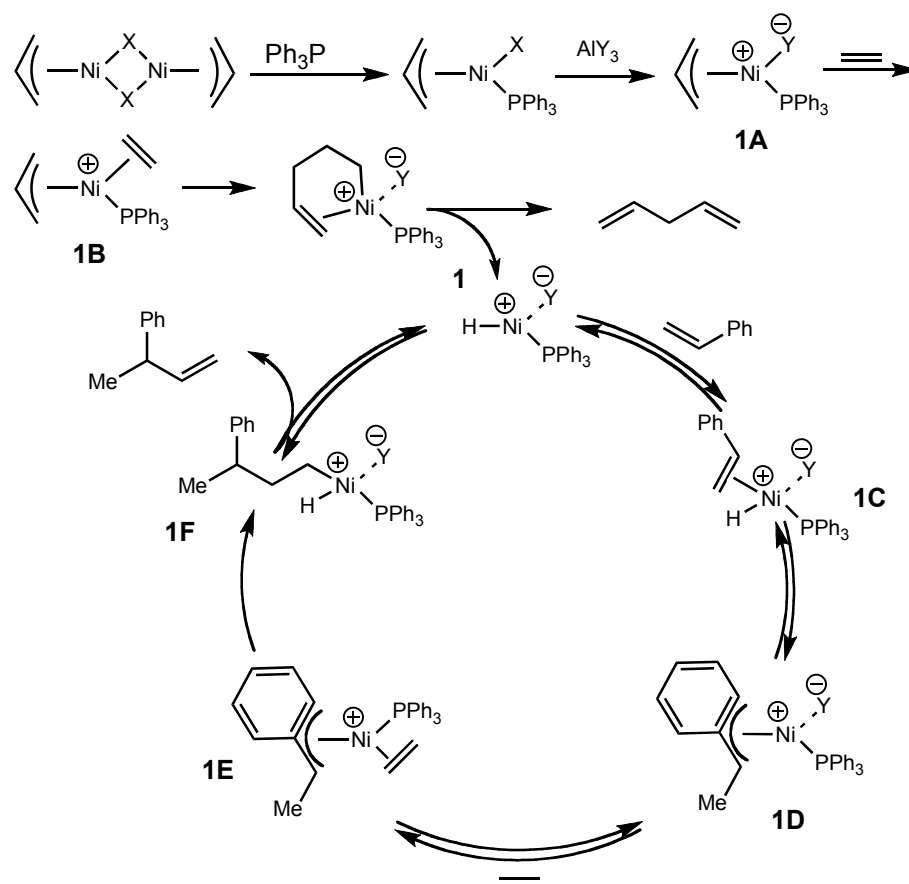


1.2 Mechanism of the Hydrovinylation Reaction

The accepted mechanism for the hydrovinylation reaction involves a cationic nickel hydride species associated with a weakly coordinating counterion, **1** (Scheme 2).¹ In order for this to occur, **1** is generated *in situ* by the Lewis acid promoted (e.g. Et_3AlCl_2) dissociation of the nickel halide bond to open a coordination site (**1A**) followed by association of either ethylene or styrene (**1B**). This is then followed by a beta-hydride elimination forming **1**. After generation of **1**, association of styrene (**1C**) followed by migratory insertion of the hydride (following Markovnikov's rule) to styrene gives a stabilized η^3 -complex (**1D**), followed by ligand association of ethylene (**1E**).

This intermediate then undergoes migratory insertion (**1F**) and β -hydride elimination to regenerate **1** and the hydrovinylation product.

Scheme 2

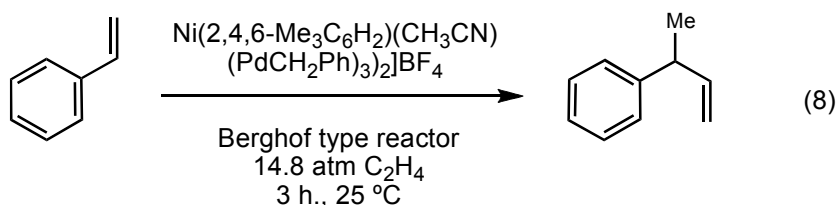


Although the hydrovinylation reaction has been known since the early 1960's,⁵ it has not been developed into a commonly used transformation for synthetic organic chemists. The drawbacks to the recently developed hydrovinylation catalyst systems are the use of starting materials in order to generate an active catalyst *in situ*. Due to the nature of this protocol, problems will exist (e.g. loss of starting material) when attempting to perform an intramolecular hydrovinylation reaction. Another drawback is the issue of Lewis acid activation. Substrates containing heteroatoms tend to show poor

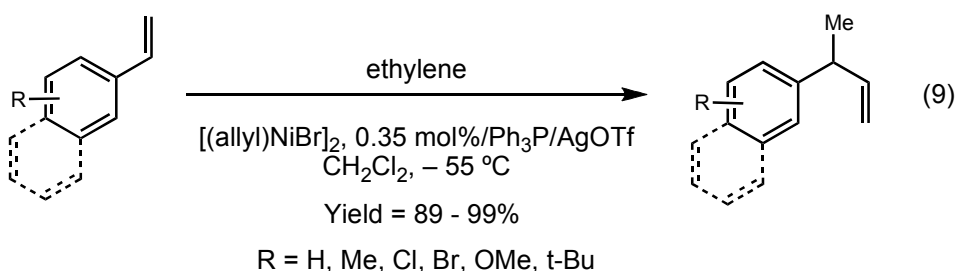
reactivity due to association between the metal center and Lewis basic sites. There is also a loss of reactivity of electron deficient vinylarenes due to a low rate of metal hydride addition. Finally, chelating, bidentate phosphine ligands inhibit the reaction due to nickel's favored 16-electron square planar geometry. This can be explained with two important intermediates shown in Scheme 2 (**1C** and **1E**). Before association of the olefin can occur, generation of **1** must occur *in situ*. This opens a coordination site allowing the olefin to associate to the metal center. After the migratory insertion of the hydride, another olefin associates to nickel (**1E**) allowing two olefins on the metal center in the same time. If a chelating bidentate ligand is used the reaction will not proceed due to the lack of an open coordination site for olefin association.

1.3 Nickel and Palladium Catalyzed Reactions

To further explore the hydrovinylation reaction, Kawata^{6,7} and co-workers used a catalyst system based on a bis(triphenylphosphine) σ -aryl(bromo)nickel(II) and boron trifluoride in methylene chloride. The codimerization took place at 0 °C under atmospheric pressure to give 3-phenyl-1-butene. By modifying this catalytic system, Muller^{16,17} observed that $[\text{ArNi}(\text{PR}_3)_2(\text{MeCN})]^+ \text{BF}_4^-$ (Ar = mesityl, R = benzyl) could serve as an efficient catalyst system for the hydrovinylation of styrene and ethylene. With high turnover rates (1915 h^{-1}) observed in THF under 15 atm of ethylene, electron rich and poor styrenes were coupled to ethylene quite well with the exception of the *p*-nitrostyrene showing very low reactivity for codimerization. The catalytic system Muller developed also avoided problems observed with boron trifluoride and other Lewis acids that give rise to polymerization (eq 8).



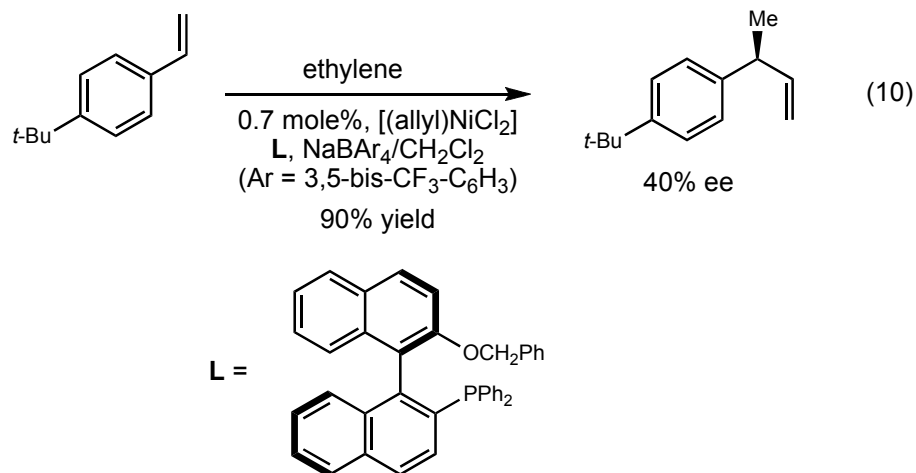
In 1998, Rajanbabu¹⁸ and co-workers reported a catalyst system composed of $[(\text{allyl})\text{NiBr}]_2/\text{Ph}_3\text{P}/\text{AgX}$ ($\text{X} = \text{OTf}$ or $\text{Ar}'_4\text{B}^-\text{Na}^+ = \text{NaBArF}$) in methylene chloride to perform the hydrovinylation of vinyl arenes and ethylene (eq 9). A variety of vinylarenes provided yields greater than 90% conversion and under these conditions no oligomerization of either the vinylarene or ethylene was detected.



Typically, vinylarenes containing Lewis basic sites are not reactive under these conditions.^{1,2} Application of this methodology to substrates such as 4-isobutylstyrene and 2-methoxy-6-vinylnaphthalene, precursors of important anti-inflammatory agents, gave very high yields of the desired hydrovinylation products.

The catalytic system can be adapted for an asymmetric reaction with the use of monodentate chiral phosphine ligands. The use of Hayashi's¹⁹ 2-diphenylphosphino-2'-methoxy-1, 1'-binaphthyl (MOP) ligand was very important in attaining 40% ee (eq 10). Hayashi's ligand contains an auxiliary group ($-\text{OCH}_2\text{Ph}$) suggested to help stabilize²⁰ the cationic intermediates by internal coordination. Without this hemi-labile group, the yield and enantioselectivity dropped to 13 and 3%, respectively. Even though the

enantioselectivity for this reaction is somewhat low, these important results were to become the backbone of the asymmetric hydrovinylation reaction.



As a heavy contributor to the development of the hydrovinylation reaction, Rajanbabu has been able to adapt his protocol to many different types of monodentate ligands in efforts to fine-tune his catalyst system. This flexibility has allowed the use of biaryl and amino moieties of Feringa's phosphoramidite ligands²¹ that are structurally simpler, yet more efficient and selective ligands for asymmetric hydrovinylation of vinylarenes (Fig 1).²²

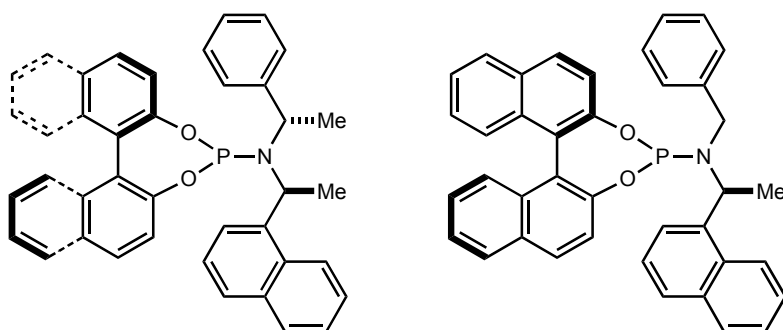
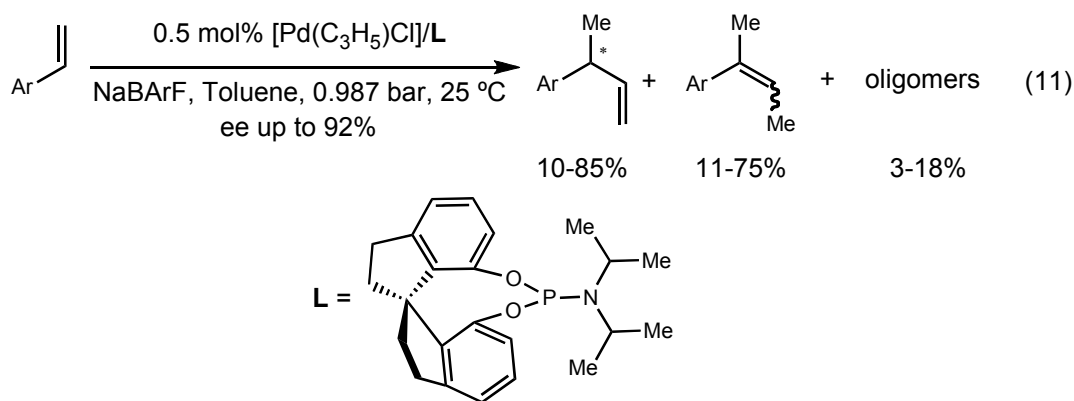


Figure 1. Derivatives of Feringa's phosphoramidite ligands

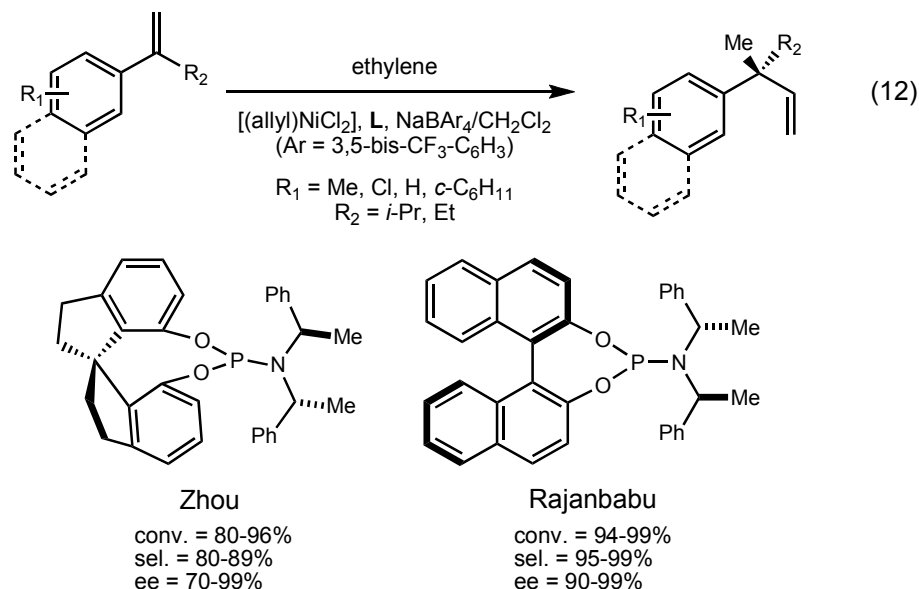
In all cases, including styrenes with lewis basic sites, when using the phosphoramidite ligands, exceptionally high yields, selectivity and enantioselectivities (>99% conv, >99% sel., 94-99% ee) of the 3-arylbutenes were reported for olefin hydrovinylation.

Other available transition-metal catalysts based on cobalt, palladium, and iridium have been used for the hydrovinylation reaction. All reactions suffer from limited substrate scope, and many exhibit various problems related to the high reaction temperatures and product isomerization (e.g., 3-phenyl-1-butene to 2-phenyl-2-butene) and/or oligomerization of styrene or ethylene (eq 11). Typically Pd-catalyzed reactions give linear products with extensive isomerization, but under special conditions, selectivity is possible to obtain the desired hydrovinylation product.



For example, Zhou²³ and co-workers used a catalyst system composed of $[\text{Pd}(\eta^3\text{-C}_3\text{H}_5)(\text{COD})]\text{BF}_4$, chiral spiro phosphoramidite and/or phosphite ligands in methylene chloride, 9.87 atm of ethylene at 25 °C to form the desired 3-arylbutenes as well as isomerization of the terminal olefin and oligomers (up to 86% conv., 26-83%, 4-73%, 1-16% sel, up to 38% ee). Under optimal conditions, (use of NaBArF, 0.987 atm of

ethylene at 25 °C in toluene) the reaction time, yield, selectivity and enantioselectivity was improved (eq 11). Enantioselectivity for this catalytic system using their developed chiral phosphoramidite ligand showed good results, but ultimately the reaction protocol still suffered from side reactions.



The chiral spiro monophosphoramidite ligand developed in Zhou's lab allowed Zhou and co-workers to broaden the hydrovinylation reaction of vinylarenes to α -alkyl vinylarenes (eq 12).²⁴ With these conditions a variety of α -alkyl vinylarenes were successfully hydrovinyolated to form new arene compounds all bearing quaternary stereocenters. It was observed that substrates with electron-withdrawing groups at *para* or *meta* positions gave products in quantitative yield, while compounds bearing electron-withdrawing groups lowered the yield to 77%. Styrenes with Lewis basic sites, for example 4-methoxystyrene and 3-methoxystyrene, show excellent selectivity and enantioselectivity for the reaction (84-89% sel., 98% ee). Rajanbabu's catalyst system²⁵ has advantages in efficiency and practicality, including both the commercial availability

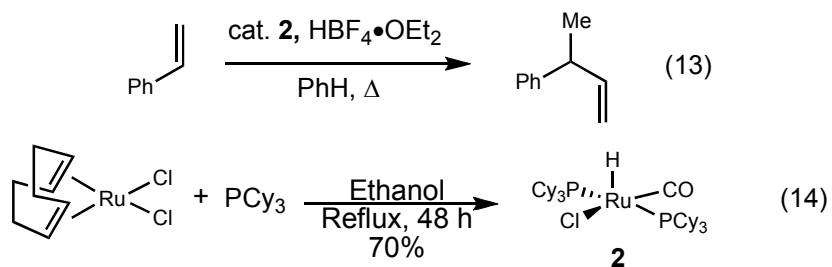
of the chiral ligand employed (Feringa's ligands), and the enantioselectivity achieved. But his catalytic system did not test whether or not Lewis basic sites affect the outcome of the hydrovinylation reaction.

Many monodentate ligands are designed with the purpose to increase the yield, selectivity and enantioselectivity in the hydrovinylation reaction. Nevertheless, the substrate scope is still limited to vinylarenes and 1,3-dienes.

1.4 Ruthenium Catalyzed Reactions

Although nickel and palladium catalysts are used more frequently due to their reactivity in catalyzing this particular reaction, ruthenium II chloride was one of the first metals to catalyze the dimerization of ethylene (eq 4).⁵

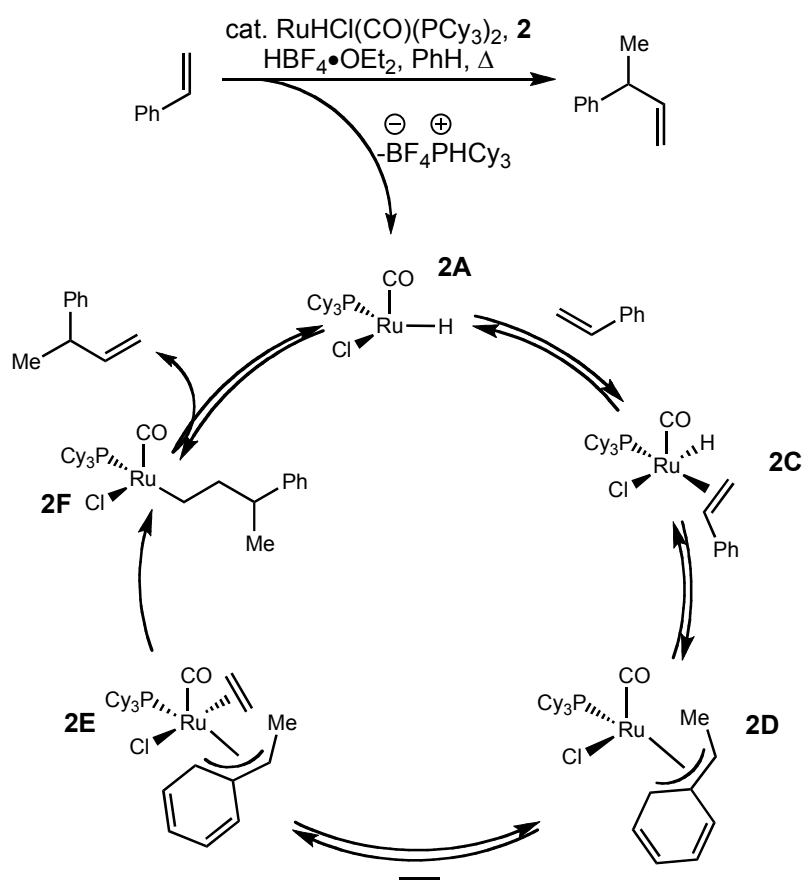
Unfortunately, other ruthenium complexes show little to no activity as catalysts in these reactions.^{12,26} However, Yi and co-workers reported that a pentavalent ruthenium hydride complex, $\text{RuHCl}(\text{CO})(\text{PCy}_3)_2$ (**2**), when treated with $\text{HBF}_4 \cdot \text{OEt}_2$ and heated, catalyzed the hydrovinylation reaction of styrene and ethylene with good yield and selectivity (eq 13).²⁷⁻²⁹ The ruthenium hydride complex **2** is convenient to use, as it can be isolated and stored and is moderately tolerant to air and water (eq 14).



Mechanistically, $\text{HBF}_4 \cdot \text{OEt}_2$ acts as a strong acid to protonate a dissociated tricyclohexylphosphine ligand (Scheme 3), which opens a coordination site on the

ruthenium metal providing an active neutral catalyst species (**2A**). This allows styrene to associate to the metal center (**2C**), followed by a migratory insertion of the hydride to give an η^3 -complex (**2D**). Next, association of ethylene (**2E**) followed by migratory insertion giving **2F**. This is then followed by beta-hydride elimination to produce the desired product and reintroduce **2A** back into the system.

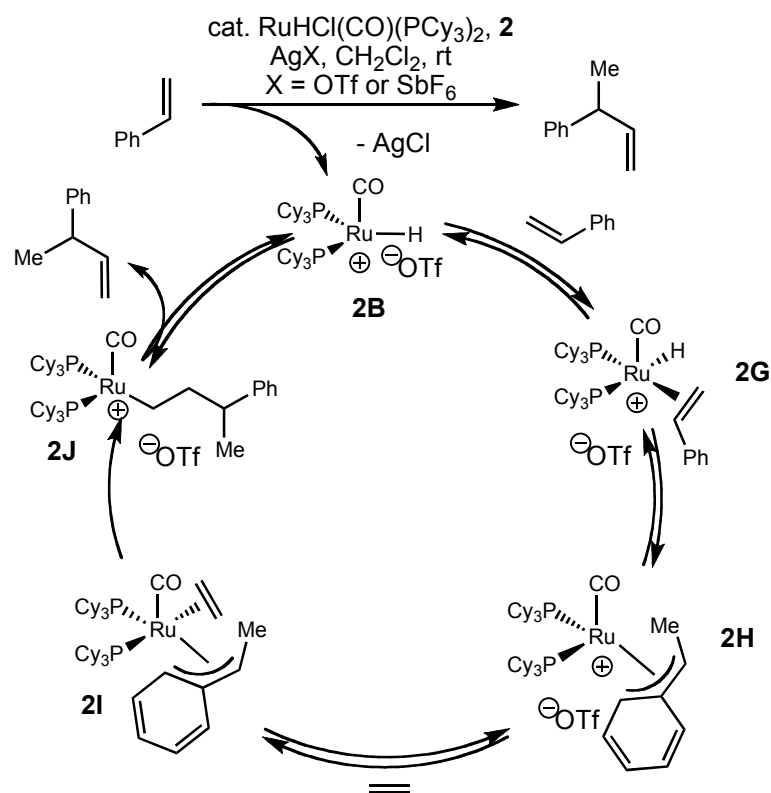
Scheme 3. Neutral Catalytic Cycle of the Hydrovinylation Reaction



1.5 Specific Aim

The aim of this project was to develop a catalyst system featuring a chiral catalyst capable to enantioselectively construct carbon-carbon bonds between ethylene and a variety of vinylarenes.

Our efforts have recently focused on the development of a cationic ruthenium complex to catalyze the hydrovinylation reaction (Scheme 4). It was envisioned that selective removal of the chloride from **2** would produce a cationic catalyst (**2B**) that may be stabilized by use of a weakly coordinating anion (e.g., OTf, SbF₆).² The cationic catalyst would then undergo association with styrene (**2G**) followed by a migratory insertion of the hydride to give a stabilized η^3 -complex (**2H**) similar to that shown in Scheme 3. Next, association of ethylene (**2I**), migratory insertion, followed by beta-hydride elimination (**2J**) would give the desired product and regeneration of **2B**. This method of activation would avoid the use of a strong acid to activate the catalyst and the need to heat the reaction mixture above room temperature (Scheme 3), thereby allowing a more versatile protocol which may be amenable to milder reaction conditions and hence a larger substrate scope.

Scheme 4. Cationic Catalytic Cycle of the Hydrovinylation Reaction

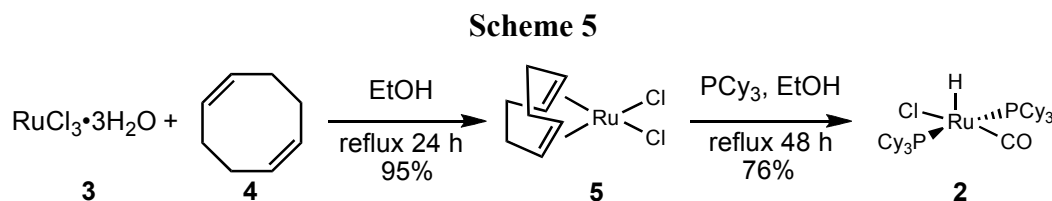
Another advantage of this process is the continued presence of two phosphine ligands on the metal center throughout the catalytic process. These ligands could presumably be replaced with a chelating chiral bis(phosphine) to deliver a chiral, nonracemic catalyst. Chelating ligands cannot be utilized with the known nickel and palladium catalysts, as they block an open coordination site needed for olefin coordination in these systems. The mechanistic pathway shown in Scheme 2 explains the reason behind this concept (Scheme 2, **1C** and **1E**).

CHAPTER II

**INVESTIGATION OF A RUTHENIUM-BASED CATALYST SYSTEM FOR
THE HYDROVINYLATION REACTION***

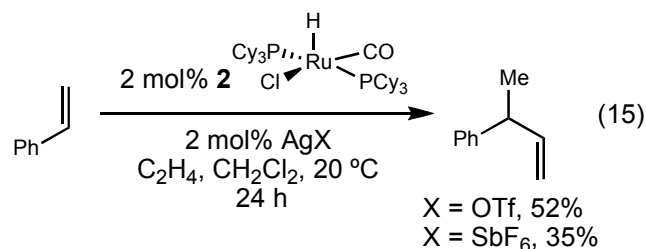
2.1 Initial Study and Application

Efforts into making the $\text{RuHCl}(\text{CO})(\text{PCy}_3)_2$ **2**, was done using a known procedure by Chae *et al* $\text{RuCl}_3 \cdot 3\text{H}_2\text{O}$ (**3**) was treated with 1,5-cyclooctadiene (**4**) in absolute ethanol to yield 95% of $\text{RuCl}_2[\text{COD}]_n$ (**5**). This air-stable ruthenium (II) complex was then treated with tricyclohexylphosphine in ethanol and refluxed for 48 hours under argon to give **2** in 76% yield as a fine yellow powder (Scheme 4).



We initially screened a variety of silver salts in combination with **2**, for the hydrovinylation of styrene under a 1 atm pressure of ethylene. For example, treatment of styrene with ethylene in the presence of **2** and AgSbF_6 in CH_2Cl_2 gave 3-phenylbutene in 35% yield after 24 h at room temperature (eq 15). Utilizing the triflate counterion (OTf) increased the yield to 52%. Other anions, including ClO_4^- and BF_4^- , were less effective.

* Reproduced with permission from “A Ruthenium based Catalyst System for Hydrovinylation at Room Temperature” by Richard Sanchez, Brian Connell, 2008, *Organometallics*, **27**, 2902-2904, Copyright 2008 American Chemical Society



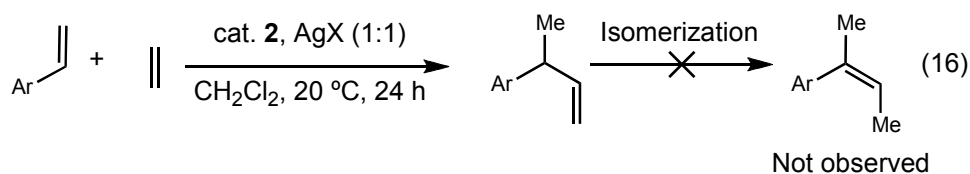
The scope of this reaction protocol was examined further by reacting ethylene with a variety of vinylarenes, catalyst **2**, and either AgOTf or AgSbF₆ (Table 1). All reactions were allowed to proceed for 24 h for the sake of comparison, although some reactions were complete in significantly less time. In some instances, lowering the catalyst loading to 0.5 mol% helped to increase the yield (entries 1 and 2). In the case of 4-methoxystyrene (entry 2), only polymerization resulted when 2 mol % of **2** was used with the SbF₆ counterion. Lowering the catalyst loading to 0.5 mol% produced 45% of the hydrovinylation adduct without signs of polymerization. Finally, replacing AgSbF₆ with AgOTf dramatically increased the yield of the desired product to 99%. There are both electronic and steric effects noticeable in these reactions; however, in most cases very good yields are still possible (entries 4-6). Steric effects appear to effect the formation of the desired compound in a more profound manner. This is possibly due to the formation of the η^3 intermediate formed during the reaction sequence (Scheme 4, **2H**). As the substituent on styrene is moved from the para to meta position, repulsion is amplified due to an increase in the steric nature of the transition state arrangement with the addition of the other olefin on the metal center (Scheme 4, **2I**).

Table 1. Hydrovinylation of Vinylarenes Catalyzed by **2**/AgX

$\text{Ph-CH=CH}_2 \xrightarrow[\text{2 mol\% AgX, C}_2\text{H}_4, \text{CH}_2\text{Cl}_2, 20^\circ\text{C, 24 h}]{\text{2 mol\% 2}}$
 Ph-CH(Me)-CH=CH_2

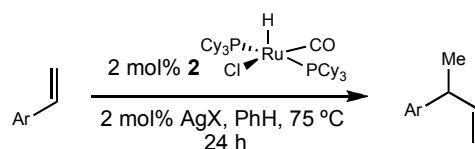
Entry	Product	2 (%)	X	Yield (%)	ref.
1		0.5	OTf	98	40
		2.0	OTf	52	
2		0.5	OTf	99	40
		0.5	SbF ₆	45	
3		0.5	OTf	67	41
		2.0	OTf	81	
4		2.0	SbF ₆	60	40
5		0.5	OTf	60	40
		2.0	SbF ₆	96	
6		0.5	OTf	18	42
		2.0	SbF ₆	75	
7		0.5	OTf	23	40
		2.0	OTf	88	

As for the electronic effects observed in this catalyst system, Lewis basic sites on styrene did not affect the outcome of the reaction (entry 2), while electron poor styrenes produced lower product formation. When using 4-nitrostyrene, only traces were observed due to a solubility problem. Gratifyingly, we never observed olefin isomerization of the products (eq 16).



Ruthenium hydride catalyst **2** can be made in one step, isolated, and stored. Complex **2** requires only treatment with a nonacidic Ag salt to become an active catalyst, rather than the strong Brønsted or Lewis acids required in other systems. The system works under mild conditions, at room temperature, and at atmospheric pressure. The possibility now exists to use chelating, bidentate phosphine ligands in this reaction process.

As aforementioned, drawbacks to the hydrovinylation reaction keep it from being an excellent tool for organic chemists; it is not only the designed protocols used to generate the catalysts but also the small substrate scope used for this particular reaction. Most substrates used for the hydrovinylation reaction are styrene based with the most common ring substitutions being either halogens, ethers or alkyl groups. In efforts to broaden the substrate scope we used our protocol on different styrene derivatives and heterocycles shown in Table 2.

Table 2. Hydrovinylation of Vinylarenes and Indole Derivatives Catalyzed by **2**/AgX

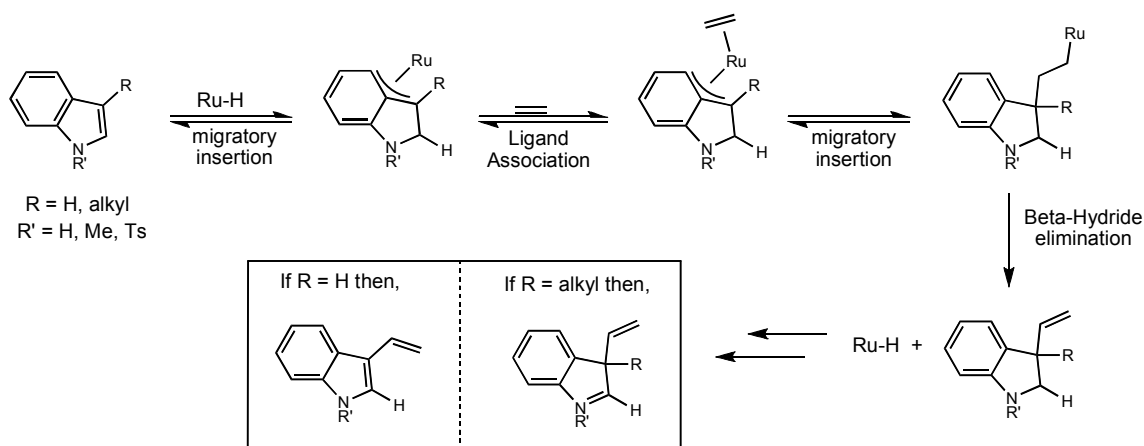
Entry	Substrate	2 (%)	X	Outcome	Entry	Substrate	2 (%)	X	Outcome
1		2.0	OTf	NR	7		2.0	OTf SbF ₆	NR
2		2.0	OTf	NR	8		2.0	OTf SbF ₆	NR
3		2.0	SbF ₆	NR	9		2.0	OTf SbF ₆	NR
4		2.0	SbF ₆	NR	10		2.0	OTf SbF ₆	NR
5		2.0	SbF ₆	NR	11		2.0	OTf SbF ₆	NR
6		2.0	OTf SbF ₆	NR					

Under Dr. Yi and co-workers' protocol, methyl cinnamate (Entry 1) gave a mixture of isomers. Our catalyst system also proved to be inadequate for this particular substrate. Substitution at the benzylic position of styrene (entry 2) completely inhibited the reaction from occurring. This led us to believe that steric interactions played a significant role in this particular substrate. Entries 3, 6 and 9 showed no product formation due to the possibility that these compounds act better as ligands with the ruthenium metal center. While trying to explore different substrates for the hydrovinylation reaction, expanding towards heterocycles was our next option. Before

using 3-vinylindoles, our reaction conditions were tested on indole and protected indoles (Me, Ts).

We envisioned the metal center coordinating to the indole, migratory insertion of the hydride would occur at the 2 position. Next association of ethylene followed by migratory insertion to re-aromatize the phenyl ring, which would then undergo a β -hydride elimination to give the desired olefin.

Scheme 6. Proposed Hydrovinylation Reaction Mechanism of Indoles



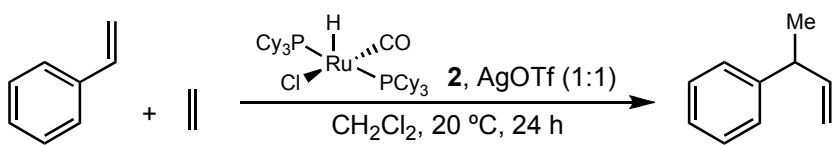
Unfortunately all attempts to perform the hydrovinylation on 3-H-indole failed. Even N-methyl and N-tosyl indole substrates did not show signs of product. We then attempted the hydrovinylation reaction on 3-vinyl indole and its protected analogues (entries 9, 10 and 11). Again heating these reactions did not have any affect on the outcome of the reactions; only starting materials were observed.

2.2 Mode of Deactivation

As several (but not all) reactions exhibited an increase in yield with a lowering of catalyst loading, we briefly examined the effect of concentration of the catalyst on the yield of the hydrovinylation of styrene with ethylene. In order to test this

experimentally, we varied the concentration of **2** while keeping the concentration of styrene constant (Table 3).

Table 3. Effect of Catalyst Concentration



Entry	styrene Conc. (M)	amt of 2 (%) ^a	2 Conc. (M)	Yield (%) ^b
1	0.96	0.5	0.0048	60
2	0.96	0.25	0.0024	74
3	0.24	0.5	0.0012	98
4	0.24	2.0	0.0048	52
5	0.24	1.0	0.0024	75

^a Catalyst loading. ^b Yield by GC.

In entries 1 and 2 it is observed that as the concentration of **2** decreases (0.0048 M to 0.0024 M), an increase in product yield (60 to 74%) is obtained. Entries 3 – 5 provide stronger evidence in the concentration dependency of **2**, for the reason that, as the concentration decreases even further (0.0024 M to 0.0012 M) the desired product yield increases to 98%. Due to these observations, it is possible that the catalyst can form a dimer by bridging between the chloride atoms when the concentration of **2** is high in the reaction (**Fig. 2**).

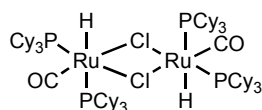


Figure 2. Possible Bimolecular Decomposition Model in Reaction

This bridging creates a more stable complex as it goes from a 16 to an 18-electron species. Another possible dimer to allow for stabilization to occur would be the bridging between two carbonyl groups, due to their π -backbonding capabilities. By understanding these two possible outcomes, bimolecular decomposition is a plausible mode of deactivation in this system. As observed through this small study, if you can optimize the concentration of catalyst used, catalyst deactivation can be avoided. Further studies are necessary to fully explore this effect, which will aid in future catalyst development.

CHAPTER III

INTRODUCING CHELATING, BIDENTATE PHOSPHINE LIGANDS TO THE RUTHENIUM METAL CENTER

3.1 Bidentate Phosphine Ligands

Recent studies have been directed toward designing new catalysts (**Figure 3**) for asymmetric olefin hydrovinylation between vinylarenes and ethylene. The catalyst design incorporates the use of chelating, bidentate phosphine ligands as our source of asymmetry.

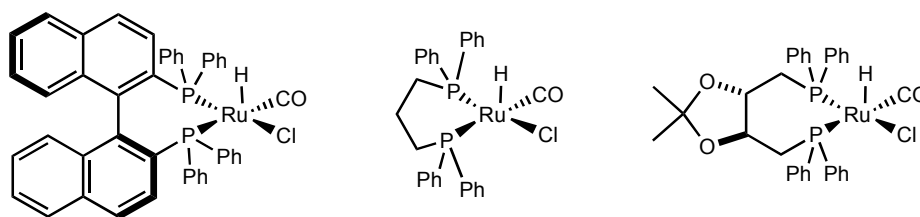
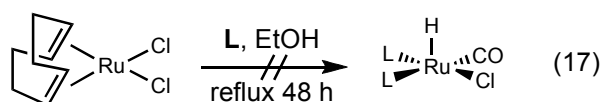


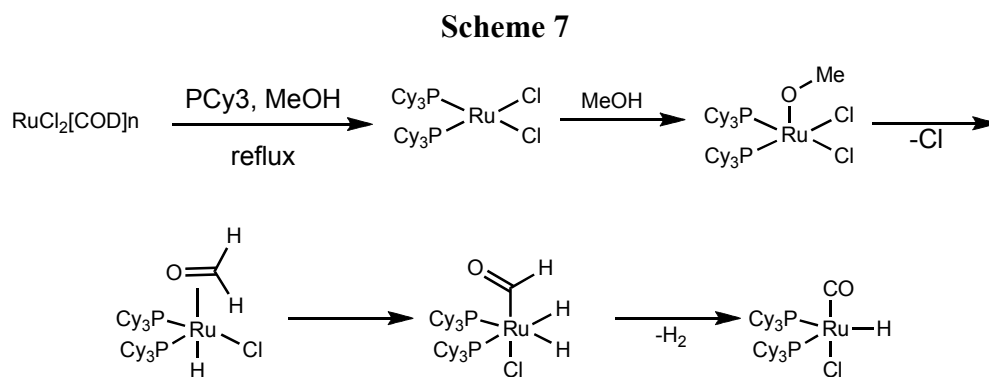
Figure 3. Design of New Pentavalent Ruthenium Hydride Complexes

Because pentavalent ruthenium hydride complexes shown above have not been synthesized, a simple protocol is needed to screen a variety of ligands that can be purchased or synthesized quickly and easily. Unfortunately, the same protocol used to synthesize **2** (eq 17) did not produce the desired complexes.

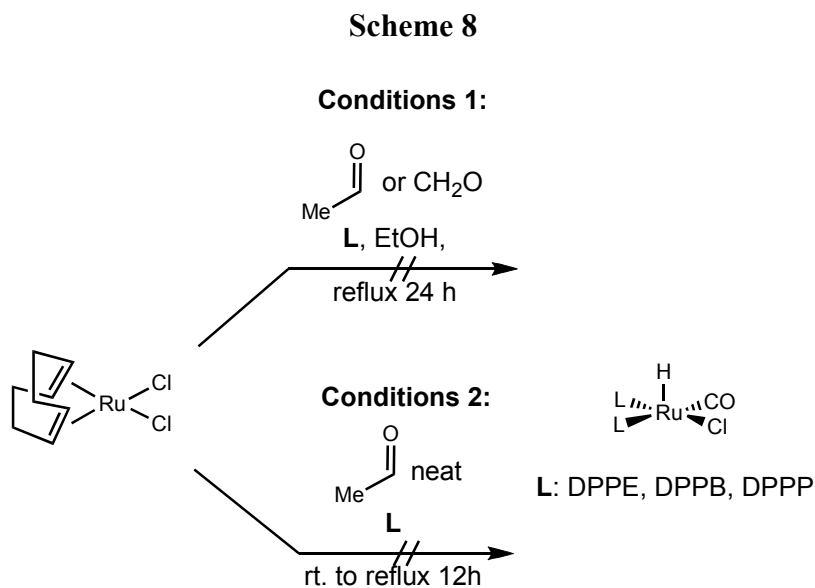


L: DPPE, DPPB, DPPP, DIOP, BINAP
Trost Ligand, Josiphos

A proposed mechanism to generate **2** is shown in Scheme 7. A small amount of acetaldehyde was observed while preparing catalyst **2**. Therefore, in attempt to place bidentate ligands on the metal center along with the hydride and carbonyl needed for the catalyst system, acetaldehyde and formaldehyde were used to push the equilibrium toward product formation.

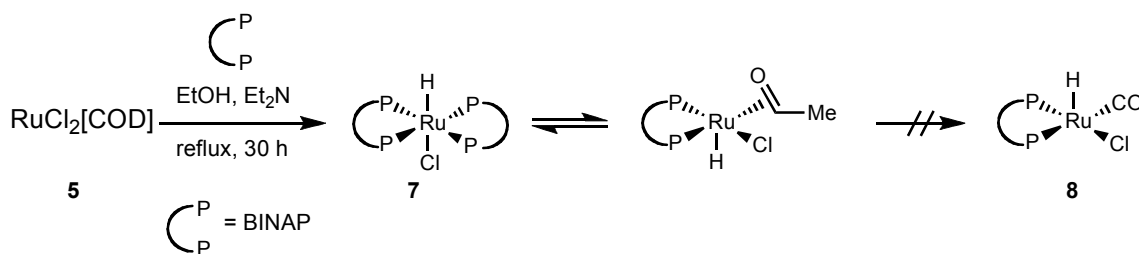


Using 10 to 20 equivalents of acetaldehyde or formaldehyde in an ethanol solution proved to be unsuccessful. An attempt to use neat acetaldehyde showed the same results (Scheme 8).



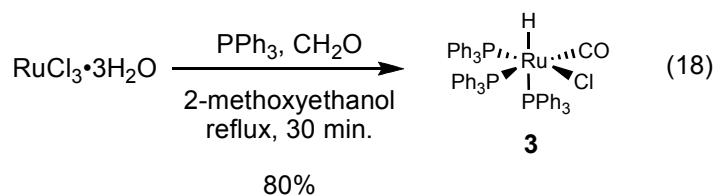
As an ongoing effort to develop a simple protocol to place commercially available ligands on the ruthenium metal center, Kawano and co-workers³⁰ published a synthesis of a ruthenium (II) bis-BINAP hydride complex **7** (Scheme 9). The idea for this approach was to form **7**, then as BINAP dissociated from ruthenium, hydride formation and carbonylation would occur to afford **8** (Scheme 9). A series of reactions were done observing the presence of hydride species being generated. The reaction was scaled up to observe carbon NMR and IR. No carbonyl peaks were observed for these complexes.

Scheme 9

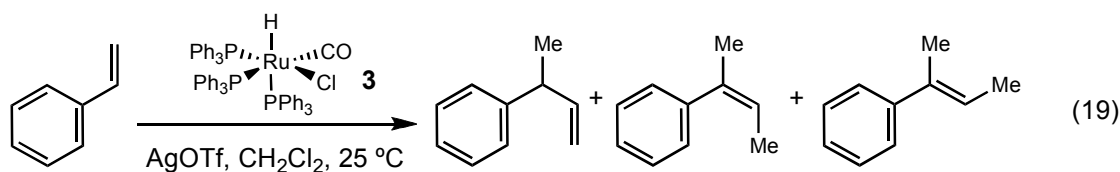


3.2 RuHCl(CO)(PPh₃)₃ as a catalyst for the Hydrovinylation Reaction

To further understand the chemistry behind the desired ruthenium hydride complexes, RuHCl(CO)(PPh₃)₃ (**3**) was used as a starting point. This catalyst is commercially available, but can also be prepared easily in one step:³¹ to a boiling solution of triphenylphosphine in 2-methoxyethanol, was added RuCl₃•3H₂O and aqueous formaldehyde successively. The reaction mixture was refluxed for 30 minutes and then allowed to cool to room temperature. Compound **3** was isolated as a moderately air stable creamy white solid in 80% yield (eq 18).

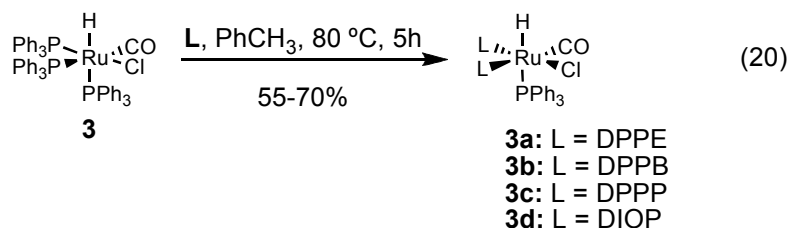


Using our optimized protocol, formation of the desired 3-arylbutene as well as isomerization of the olefin was observed (eq 19). We also set out to optimize reaction conditions that would allow only the formation of 3-arylbutenes; unfortunately, this catalytic system did not provide the desired selectivity.



3.3 Synthesis of Modified Ruthenium (II) Hydride Complexes

To synthesize a modified version of **3**, aryl bidentate ligands were used (e.g. DIOP, BINAP). A known procedure by Moo-Jin and co-workers³² was implemented to coordinate these types of ligands on the metal center. To prepare the modified complexes, a solution of **3** in toluene was charged with a bidentate ligand and heated at 80 °C for 5 hours. Products were isolated as a creamy white solids yielding 55 to 70% (eq 20). On the other hand, BINAP did not coordinate with the metal center. These complexes were synthesized because of the ease of screening a variety of bidentate phosphine ligands.



When these complexes were submitted to the reaction conditions only starting materials were isolated. To rationalize these observations, mechanistically, two coordination sites are required (**2I**, Scheme 4). This allows the binding of both olefins to occur. The extra triphenylphosphine ligand occupies a considered necessary site for olefin association, inhibiting the reaction from progressing forward. In an attempt to open a coordination site, copper (I) chloride was used as a phosphine scavenger. Only starting materials were isolated.

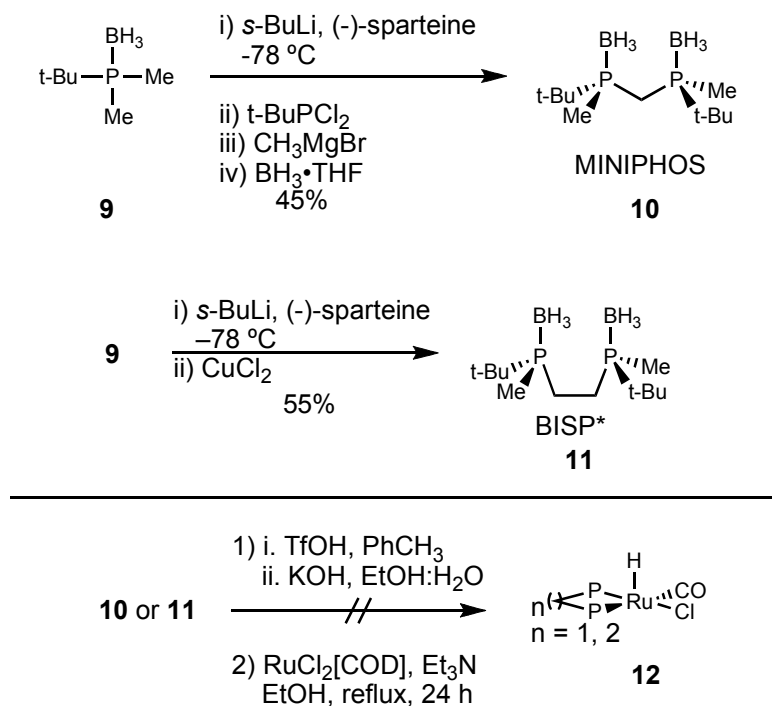
3.4 Chelating, Bidentate Phosphine Borane Ligands

In order to synthesize a catalyst, it is crucial that the ligands chosen be electron rich and sterically hindering enough to stabilize the formation of hydride complexes. Prior attempts to use chelating, bidentate phosphine ligands containing aryl substituents (e.g. BINAP, DIOP, DPPE, DPPP, DPPB, TROST Ligand) with the standard protocol ($[\text{RuCl}_2(\text{COD})]_n$ refluxed in ethanol) to synthesize **2** led to unsuccessful results.

Imamoto and co-workers in 1998 and 1999, developed chiral chelating phosphine ligands containing electron rich alkyl groups known as MiniPHOS (**10**)³³ and BisP* (**11**)³⁴ (Scheme 10). These ligands are air stable, due to the presence of the borane protecting group. Compound **9** was prepared in three steps from phosphorous trichloride, and then treated with *s*-BuLi/(-)-sparteine, *t*-butyldichlorophosphine, methylmagnesiumbromide and $\text{BH}_3 \cdot \text{THF}$ sequentially to provide **10** in 45% yield.

Compound **11** was synthesized by selective deprotonation with *s*-BuLi/(-)-sparteine with **9**, then oxidative coupling using CuCl₂ to afford **11** in 55% yield. Attempts were then made to place these ligands on ruthenium. No formation of product **12** was observed (Scheme 10).

Scheme 10

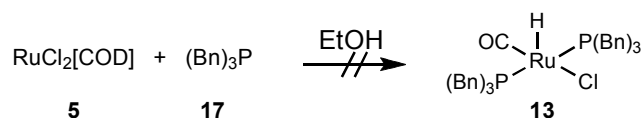


Since the alkyl groups on MiniPHOS and BisP* create such an electron rich ligand, harsh reaction conditions are needed to remove the borane from the phosphine. By replacing the methyl group with a benzyl group (basicity = tricyclohexylphosphine > tribenzylphosphine > triphenylphosphine), an amine can be used as a deprotecting agent.³⁵

Another test study was done using tribenzylphosphine. The assumption behind the use of this ligand was that like tricyclohexylphosphine (PCy₃) it is sterically

hindering enough to stabilize an open coordination site of a pentavalent complex. It is less basic than PCy₃, but more basic than triphenylphosphine³⁶. Our standard protocols did not produce **13**.

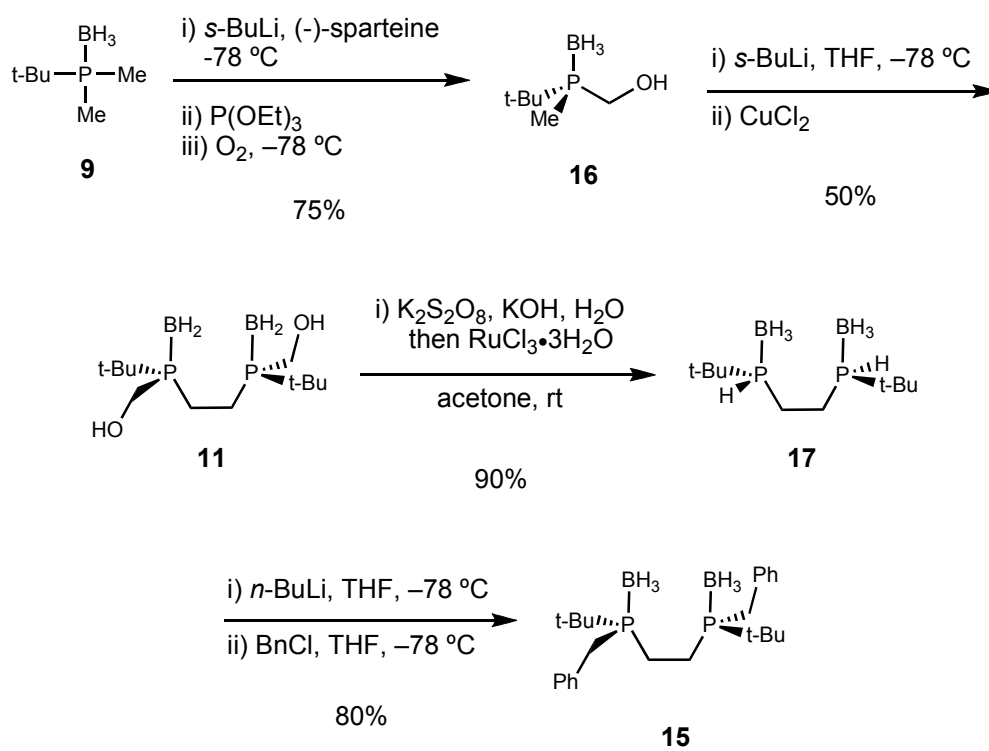
Scheme 11



It is known that bulky alkylphosphines are capable of stabilizing kinetic pentavalent ruthenium hydride complexes.³⁷ Also these ligands form hydrides to release steric strain. A review prepared by Tolman, showed that basicity, steric effects, and agostic interactions all contribute to the synthesis of pentavalent ruthenium hydride complexes³⁸. Therefore, attempting to use a more bulky derivative of **11** could be foreseen.

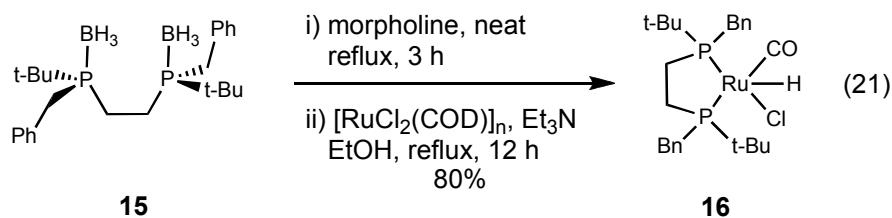
Imamoto and co-workers in 2002 published a benzyl derivative, **15**.³⁹ This derivative permitted the opportunity to simplify the deprotection step (eq 21). Compound **9** was prepared in three steps from PCl₃. It was then treated with *s*-BuLi/(–)-sparteine, triethyl phosphite, and oxygen sequentially to give **16** in 75% yield. Next, selective deprotonation with *s*-BuLi followed by oxidative coupling using CuCl₂ afforded **17** in 50% yield. After a carbon degradation sequence the phosphine-borane intermediate **18** was formed. Finally, lithiation followed by addition of benzyl chloride provided, 1,2-bis(boranato(*tert*-butyl)benzylphosphino) ethane, **15**.

Scheme 12



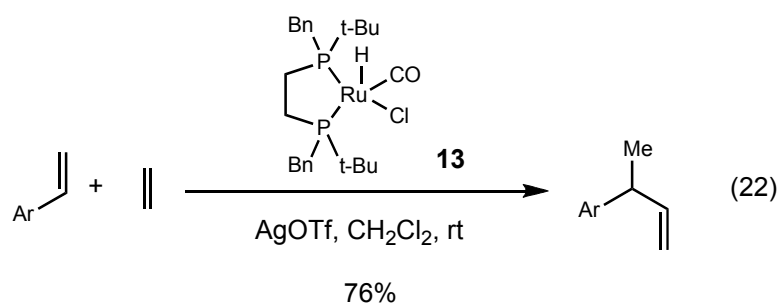
3.5 New Catalyst Featuring Chelating, Bidentate Phosphine Ligands

Having a racemic mixture of **15** in hand prior to the aforementioned synthesis, ruthenium hydride catalyst (**16**) was synthesized using $[\text{RuCl}_2(\text{COD})]_2$ and Et_3N . This mixture was refluxed in ethanol to introduce a hydride source to the metal center without the use of reducing agents or the need to generate the hydride *in situ* (eq 21).



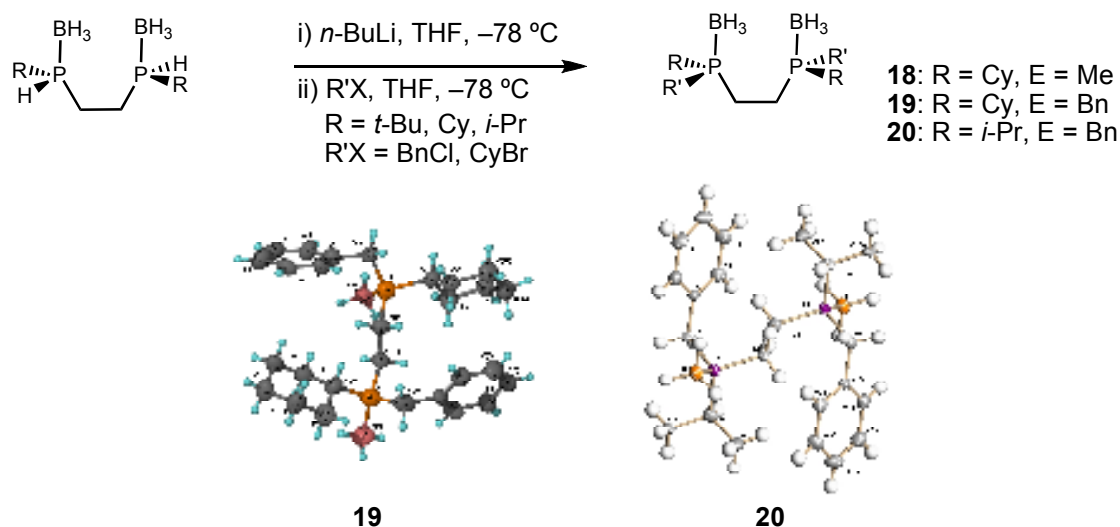
We then applied our reaction protocol to a racemic mixture of **16** to yield 76% of

the desired product after 24 h (eq 22). This is the first reported ruthenium hydride catalyst to use a chelating, bidentate phosphine ligand to promote high reactivity, selectivity and yield of the hydrovinylation reaction. Upon using a nonracemic version of this catalyst, 12% ee was observed. Lowering the temperature for this particular catalyst system inhibited the reaction from generating product. Only starting materials were isolated.



In attempt to optimize the reaction shown in eq 22, derivatives of the phosphine-borane ligand were investigated. The synthetic route to **15** allows for numerous possibilities to introduce a variety of substituents to change the steric and electronic effects governed by the ligands in order to increase the enantioselectivity of the hydrovinylation reaction. During the course of the ligand design we were able to synthesize two new phosphine-borane ligands, **19** and **20** (Scheme 13).

Scheme 13. Synthesis of phosphine-borane ligands and crystal structures **19** and **20**



The synthesis, isolation and characterization of the desired catalysts shown in Figure 4 proved to be difficult for us. Unfortunately, our proposed catalyst structures do not correlate to the carbon NMR data and IR data collected. There is no evidence of carbonyl peaks observed in either spectrum.

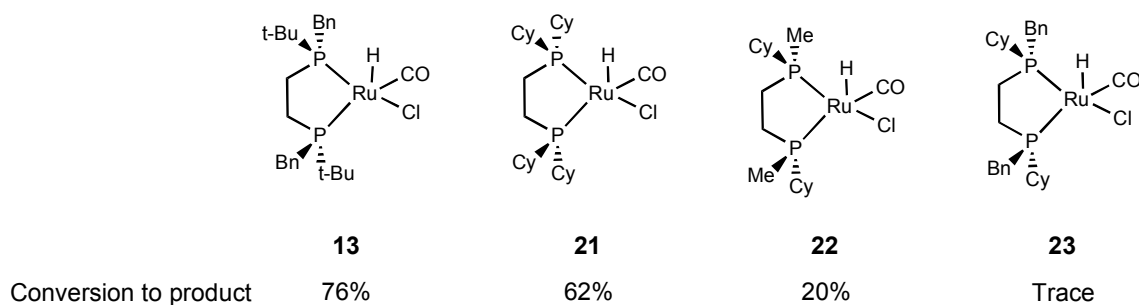


Figure 4. Desired New Active Catalysts for the Hydrovinylation Reaction

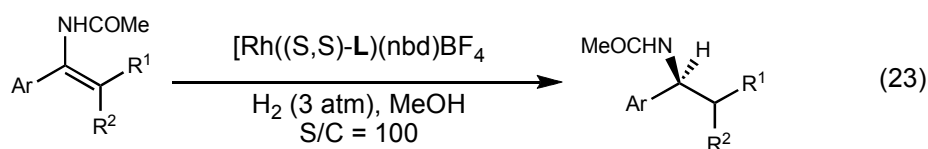
We were able to synthesize active catalysts for the hydrovinylation reaction, but because we could not grow crystals due to decomposition and/or oiling out, structure

elucidation of the ruthenium hydride catalyst was very difficult. This in turn created an immense problem when we tried to increase the enantioselectivity of the reaction.

After isolation of the unknown complex, we attempted to use it with our catalyst system protocol. Subsequent to the codimerization of styrene and ethylene took place, we observed that the selectivity for the hydrovinylation product was excellent and that the counterion used in the catalyst system affected the reaction outcome. Similar to **2**, the ligands used with these unknown catalysts are also particular towards the counter ion used. A counter ion that coordinates (OTf) more to the metal center helped to stabilize the catalyst. With a less coordinating counterion (SbF_6), the catalyst seemed to decompose rapidly. This effect is due to the complexes being very electron-rich. We also observed that removal of the *t*-butyl substituent showed a dramatic decrease in product conversion, as well as the catalysts providing racemic mixtures of the desired product.

3.6 Commercially Available Phosphine Ligands

It is known that bisphosphine ligands bearing tert-butyl group substituents demonstrate excellent enantioselectivity in transition metal-catalyzed asymmetric reactions. For example, the asymmetric hydrogenation of prochiral enamides observed by Imamoto and co-workers (eq 24).⁴⁰



Ar = Ph, 3-MeOC₆H₄,
4-MeOC₆H₄, 4-ClC₆H₄

L = *t*-Bu-BisP* - 96-99% ee
L = TangPHOS - 97-99.8% ee

R¹ or R² = H, Me

We also observed that for our catalyst system ligands containing *t*-butyl substituents increased the product formation. Therefore, we used commercially available ligands containing *t*-butyl groups as a starting point in efforts to screen for enantioselectivity (Fig. 4). In addition, we also used commercially available phosphoramidite ligands known to give excellent ee's for the hydrovinylation reaction with other metals (eq 25).

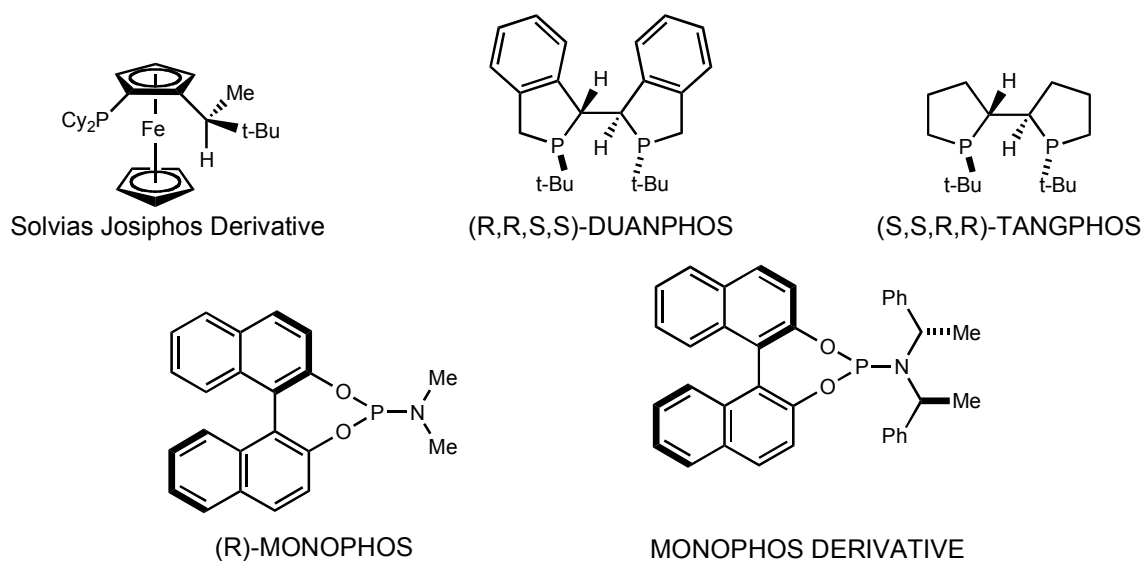


Figure 5. Commercially Available Ligands

To this end, we have been able to incorporate commercially available chelating, bidentate phosphine ligands containing tert-butyl groups in efforts to attain the steric and electronic effects needed to attain active catalysts for the hydrovinylation reaction. Unfortunately, the ligands shown in Figure 5 provided traces to moderate yielding racemic mixtures of the desired product. These active catalysts although did work for the reaction protocol were difficult to analyze due to the amount of hydrides produced and absence of carbonyl peaks during the synthesis of the catalysts.

CHAPTER IV

INVESTIGATION OF A RUTHENIUM-BASED CATALYST SYSTEM FOR
THE INTRAMOLECULAR HYDROVINYLTATION REACTION

4.1 Intramolecular Hydrovinylation Reactions

Synthesis of cyclopentanes and cyclopentenes via intramolecular hydrovinylation reaction (IHV) of 1,6-dienes catalyzed by Ru, Pd, Ni, Ti and Rh complexes has gained more attention throughout the years.⁴¹ The IHV of 1,6-dienes shows to be a very useful transformation for organic chemists in natural product synthesis, for example, tetrahydrofurans are found in a multitude of natural products such as Aureothin and Avermectin A1a (Figure 6)⁴².

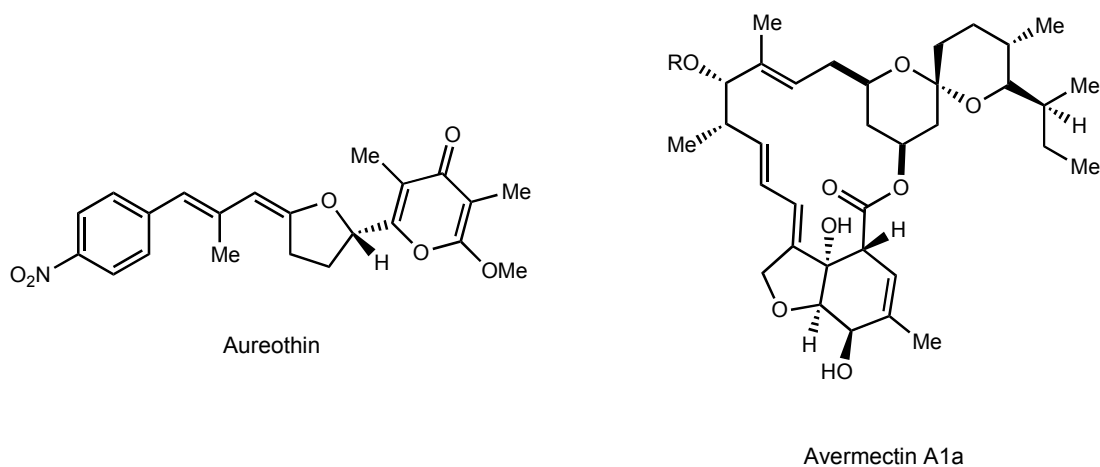


Figure 6. Natural Products: Aureothin and Avermectin A1a

Bearing in mind the precedent for a ruthenium complex to catalyze the IHV reaction and the lower reactivity 1, 6-dienes show towards transition metals; it is our endeavor to develop a more robust and easily accessible catalyst capable of catalyzing the IHV reaction with sensitive functional groups and heteroatoms.

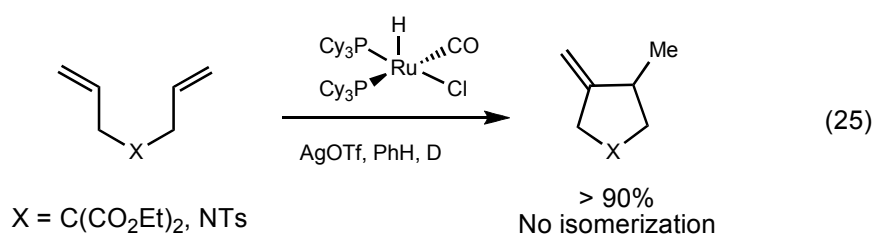
It has been reported that $\text{RuCl}_2(\text{COD})_n$ in ethanol produces these types of carbo/heterocycles via microwave,⁴³ but bidentate ligands are not compatible with catalyst system. Using the same catalyst system that evolved in our lab and using a known substrate (diallyl malonate) used in the IHV reaction, we observed after heating the reaction at 75 °C, after one hour product began form. Allowing the reaction to stir overnight produced greater than 90% yield by NMR of the desired IHV product (Table 4; entries 1 and 2).

Table 4. Intramolecular Hydrovinylation of 1,6 - Dienes Catalyzed by **2**/AgX

Substrate	Product	2 (%)	X	Yield (%)
		2.0	OTf	> 90%
		2.0	OTf	> 90%
		2.0	OTf	NR
		2.0	OTf	NR
		2.0	OTf	NR
		2.0	OTf	NR
		2.0	OTf	NR
		2.0	OTf	NR

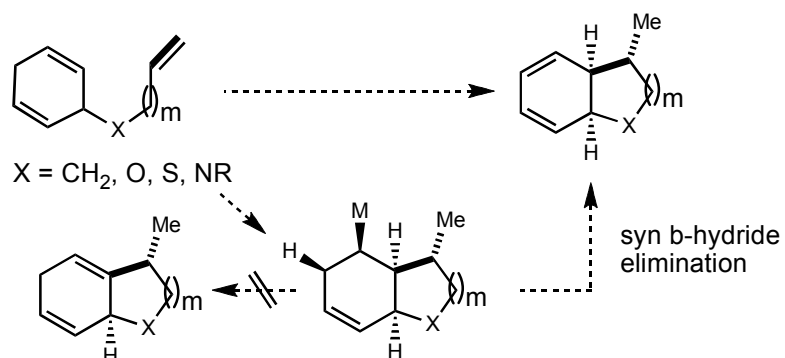
4.2 Plausible Catalytic Desymmetrization IHV Reaction

Our catalyst system has an appealing reactivity profile that leads to the desired product with no isomerization of the terminal olefin to the more stable position. Although the majority of substrates screened did not produce the desired products, entries 1 and 2 support our concept of 1 mole of starting material provides 1 mole of product.



The results shown in equation 25 also bring the possibility of a catalytic desymmetrization process shown in Scheme 14. After the formation of the carbon-carbon bond and β -hydride elimination, only one isomer can be formed. In order for this process to occur, the metal center and the hydrogen must be syn to each other producing a substrate with three syn contiguous chiral centers, the formation a Diels-Alder synthon and the formation of a carbo/heterocycle.

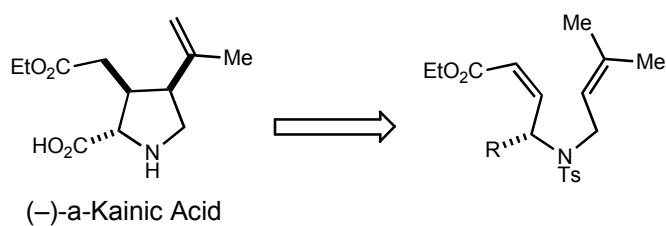
Scheme 14. Catalytic Desymmetrization Process



4.3 Natural Product Synthesis

A drawback to the previous methodology used by Yi and co-workers was that it used tetrafluoroboric acid and when combined with heat, creates a harsh reaction environment for natural product synthesis. Our catalytic system in theory can be applied towards the synthesis of natural products. A great example would be (-)- α -kainic acid.⁴⁴ This compound is a nonproteinogenic pyrrolidine dicarboxylic acid and these types of compounds have drawn big interest in the world of synthetic chemistry due to their neuropharmacological properties and structural features.⁴⁵ (-)- α -Kainic acid was isolated from *Digenea simplex* and shows potent neuroexcitatory activity in the mammalian central nervous.^{46,47}

This amino acid contains 3 contiguous stereogenic centers in the pyrrolidine ring system. What also makes kainic acid an interesting molecule is the syn relationship between the 3 and 4 position. Normally in a cyclopentane system the stereochemistry relationship is observed to be trans due to steric relief and eclipsing interactions.

Scheme 15. Retrosynthetic Analysis of (-)- α -Kainic acid

We can take advantage of an IHV reaction in this molecule by disconnecting the bond between carbons 3 and 4 to form the following 1,6-diene. This disconnection gives a compound that can first undergo model studies to see whether the possibility of having more functionality on the 1,6-diene can work as compared to entry 2 in Table 4.

CHAPTER V

CONCLUSION

In conclusion, the use of a mild and acid-free ruthenium hydride catalytic system was found to be effective for the hydrovinylation of substituted vinylarenes and 1,6-dienes at room temperature. We also developed the first hydrovinylation catalyst that provides the desired product using a chelating, bidentate phosphine ligand. Our ruthenium-based catalytic system has also proven to give an appealing reactivity profile in favor of the desired arylbutenes without promoting undesirable oligomerization and isomerization.

CHAPTER VI

EXPERIMENTAL

6.1 Experimental Section General Considerations

All hydrovinylation reactions were manipulated under argon and kept away from light, unless otherwise noted. Dry dichloromethane was used from a solvent purification system (neutral alumina, copper(II) oxide). Ethanol was distilled from sodium turnings and triethylamine and morpholine were distilled from calcium hydride prior to use and degassed using nitrogen gas. All vinylarene substrates are commercially available and were used without further purification and 1,2-Bis(dicyclohexylphosphino)ethane was purchased from Alfa Aesar. (R,R,S,S)-DuanPhos, (S,S,R,R)-TangPhos, (R)-MonoPhos, (R)-(-)-1-[(S)-2-(DicyclohexylphosphinoFerrocy] ethyldicyclohexylphosphine, (S)-(+)-(3,5-Dioxa-4-phosphacycloheptal[2,1-a;3,4a'] dinaphthalen-4-yl) bis[(1R)-1-phenylethyl]amine, (R)-Bis(diphenylphosphino)-1,1'-binaphthyl, (±)-DIOP, 1,2-Bis(diphenylphosphino)ethane, 1,2-Bis(diphenylphosphino)propane, 1,2-Bis(diphenylphosphino)butane, N,N'-(1R,2R)-1,2-Cyclohexanediylbis[2-(diphenylphosphino)benzamide] were all purchased from Strem Chemicals, Inc. Ligand Ruthenium complex **2** was prepared according to the reported procedure.²⁷ Literature procedures^{39,48} were used to prepare ligands **15** and **16**. Heating was accomplished by either a heating mantle or silicone oil bath. Temperature was controlled with a J-KEM temperature controller. Purification of reaction products was carried out by flash column chromatography using Silicycle silica gel 60 (230-400 mesh). Concentration in vacuo refers to the removal of volatile solvent using a Buchi rotary evaporator attached to a dry

diaphragm pump (10-15 mm Hg) followed by pumping to a constant weight with an high vacuum oil pump (<300 mTorr).

¹H NMR spectra were recorded on a Varian Inova 300 (at 300 MHz), or a Varian Mercury 300 (at 300 MHz), and are recorded relative to CDCl₃ (δ 7.27). ¹H NMR coupling constants (*J*) are reported in Hertz (Hz) and multiplicities are indicated as follows: s (singlet), d (doublet), t (triplet), m (multiplet), br (broad). Proton-decoupled ¹³C NMR and ³¹P spectra were recorded on a Varian Mercury 300 (at 75 MHz), and are reported relative to CDCl₃ (δ 77). High-resolution mass spectra (HRMS) were obtained at the Laboratory for Biological Mass Spectrometry at TAMU. Infrared spectra were recorded on a Bruker Tensor 27 spectrometer as thin film on NaCl plates.

6.2 Typical Reaction Procedure for the Hydrovinylation Reaction

In a nitrogen-filled glovebox, a 10 mL reaction flask equipped with a stir bar was charged with complex **2** (0.0024 mmol) and AgOTf (0.0024 mmol). The reaction mixture was removed from the glovebox, purged with argon, and charged with CH₂Cl₂. The reaction mixture was stirred for 3 h at room temperature followed by the addition of styrene (0.48 mmol) under a stream of argon. Ethylene was bubbled into the reaction flask, and a balloon was filled to maintain an atmosphere of ethylene, recharging the balloon after 12 h. The reaction mixture was stirred for 24 h total and then opened to air and filtered through a small pipette packed with silica gel (dichloromethane) to remove the metal catalyst. The product was then passed through another silica-packed pipet column (hexanes), and the solvent was removed via rotary evaporator.

(3-Phenyl-1-butene):⁴⁹ ¹H NMR (300 MHz, CDCl₃): δ 7.19-7.31 (m, 5H), 5.98-6.07 (m, 1H), 5.02-5.08 (m, 2H), 3.42-3.51 (m, 1H), 1.37 (d, $J = 6.9$, 3H). ¹³C (75 MHz, CDCl₃): 145.7, 143.4, 128.6, 127.4, 126.3, 113.3, 43.3, 20.9; MS (CI) LRMS: m/z calcd for C₁₀H₁₂ [M+H]⁺, 133; found, 133.1.

3-Naphthyl-1-butene:⁴⁹ ¹H NMR (300 MHz, CDCl₃): δ 7.3-7.80 (m, 7H), 5.98 (m, 1H), 5.10 (m, 2H), 3.64 (m, 1H), 1.46 (d, $J = 7.0$, 3H). ¹³C (75 MHz, CDCl₃): 143.2, 143.1, 133.8, 132.4, 128.2, 127.8, 127.7, 126.4, 126.1, 125.5, 125.4, 113.6, 43.4, 20.8; MS (CI) LRMS: m/z calcd for C₁₄H₁₄ [M+H]⁺, 183.0; found, 183.2.

(4-tert-butylphenyl)-1-butene:⁵⁰ ¹H NMR (300 MHz, CDCl₃): δ 7.3-7.80 (m, 7H), 5.98 (m, 1H), 5.02 (dt, $J_1 = 17.25$, $J_2 = 2.18$, 1H), 4.99 (dt, $J_1 = 10.0$, $J_2 = 2.18$, 1H), 3.39-3.49 (m, 1H), 1.38 (d, $J = 7.05$, 3H), 1.33 (s, 9H). ¹³C (75 MHz, CDCl₃): 149.1, 143.6, 142.6, 127.0, 125.5, 113.1, 42.9, 34.6, 31.6, 20.9; MS (CI) LRMS: m/z calcd for C₁₄H₂₀ [M+H]⁺, 189.0; found, 189.2.

(4-methoxyphenyl)-1-butene:⁴⁹ ¹H NMR (300 MHz, CDCl₃): δ 7.19 (d, $J = 9.14$, 2H), 6.84 (d, $J = 8.71$, 2H), 5.98 (m, 1H), 5.02 (dt, $J_1 = 17.15$, $J_2 = 1.45$, 1H), 4.99 (dt, $J_1 = 10.43$, $J_2 = 1.45$, 1H), 3.79 (s, 3H), 3.44-3.39 (m, 1H), 1.34 (d, $J = 6.99$, 3H). ¹³C (75 MHz, CDCl₃): 158.1, 143.8, 137.7, 128.3, 113.9, 113.0, 55.4, 42.5, 21.0; MS (CI) LRMS: m/z calcd for C₁₁H₁₄O [M+H]⁺, 163.0; found, 163.2.

(3-Chlorophenyl)-1-butene:⁴⁹ ¹H NMR (300 MHz, CDCl₃): δ 7.15-7.28 (m, 4H), 5.90-6.01 (m, 1H), 5.02-5.08 (m, 2H), 3.39-3.42 (m, 1H), 1.35 (d, $J = 6.9$, 3H). ¹³C (75 MHz, CDCl₃): 147.8, 142.6, 129.5, 127.6, 126.4, 113.9, 43.1, 20.7; MS (CI) LRMS: m/z calcd for C₁₀H₁₁Cl [M+H]⁺, 167.0; found, 167.1.

(4-Bromophenyl)-1-butene:⁴⁹ ¹H NMR (300 MHz, CDCl₃): δ 7.41-7.49 (m, 2H), 7.10-7.15 (m, 2H), 5.93-6.05 (m, 1H), 5.04-5.1 (m, 2H), 3.42-3.51 (m, 1H), 1.37 (d, $J = 7.1$, 3H). ¹³C (75 MHz, CDCl₃): 147.8, 142.6, 129.5, 127.7, 126.4, 113.9, 43.1, 20.8; MS (CI) LRMS: m/z calcd for C₁₀H₁₁Br [M+H]⁺, 211.0; found, 211.1.

(4-trifluorophenyl)-1-butene:⁵¹ ¹H NMR (300 MHz, CDCl₃): δ 7.55 (d, $J = 8.2$, 2H), 7.31 (d, $J = 8.0$, 2H), 5.72-6.03 (m, 1H), 5.03-5.09 (m, 2H), 3.48-3.57 (m, 1H), 1.37 (d, $J = 7.1$, 3H). ¹³C (75 MHz, CDCl₃): 149.8, 142.4, 127.6, 125.6, 125.3, 122.8, 114.2, 43.26, 20.8; MS (CI) LRMS: m/z calcd for C₁₁H₁₁F₃ [M+H]⁺, 201.0; found, 201.2.

(S,S)-1,2-bis(boranato((cyclohexyl)hydroxymethyl)phosphine)ethane: White crystals, (20% EtOAc/Hexanes) R_f = 0.46; [α]_D²³ = +1.3 (*c*, 1.0, CHCl₃); ¹H NMR (300 MHz, CDCl₃): δ 3.97-4.22 (m, 4H), 2.79 (s, 1H), 1.77-2.01 (m, 15H), 1.14-1.52 (m, 11), 0.32 (br. d, $J = 124.36$ Hz, 6H); ¹³C NMR (75 MHz, CDCl₃): 55.4 (d, $J = 33.2$), 30.6 (d, $J = 30.4$), 26.8, 26.3, 26.1, 25.6, 12.1; ³¹P NMR (121.4 MHz, CDCl₃): δ 24.4 (m)

(S,S)-1,2-bis(boranato(cyclohexyl)phosphine)ethane: White crystals, (5% EtOAc/Hexanes) R_f = 0.18; [α]_D²³ = -32.6 (*c*, 1.0, CHCl₃); ¹H NMR (300 MHz, CDCl₃): δ 4.51 (d, $J = 355.8$, 2H), 1.7-2.01 (m, 15H), 1.18-1.45 (m, 11H), 0.45 (br. d, $J = 71.7$, 6H); ¹³C NMR (75 MHz, CDCl₃): 30.6 (d, $J = 20.8$), 28.4, 27.8, 26.2, 25.5, 13.0; ³¹P NMR (121.4 MHz, CDCl₃): δ 22.6 (m).

(S,S)-1,2-bis(boranato(*i*-propyl)hydroxymethyl)phosphine)ethane: White crystals, (25% EtOAc/Hexanes) R_f = 0.38; [α]_D²³ = +1.8 (*c*, 1.0, CHCl₃); ¹H NMR (300 MHz, CDCl₃): δ 3.94-3.98 (m, 4H), 1.84 (s, 2H), 1.04-1.18 (m, 18H), 0.16 (br. d, $J = 83.9$,

6H); ^{13}C NMR (75 MHz, CDCl_3): 54.9 (d, $J=37.3$), 30.5 (d, $J=37.6$), 11.9 (d, $J=31.5$); ^{31}P NMR (121.4 MHz, CDCl_3): δ 21.5 (m).

(*S,S*)-1,2-bis(boranato(*i*-propyl)phosphine)ethane: White crystals, (5%

EtOAc/Hexanes) $R_f=0.23$; ^1H NMR (300 MHz, CDCl_3): δ 4.48(d, $J=354.8$, 2H), 1.84-2.19 (m, 4H), 1.18-1.32 (m, 14H), 0.43 (br. d, $J=92.5$, 6H); ^{13}C NMR (75 MHz, CDCl_3): 34.6 (d, $J=36.6$), 18.4, 17.5 (d, $J=32.2$), 13.5 (d, $J=30.0$); ^{31}P NMR (121.4 MHz, CDCl_3): δ 24.4 (m).

(*R,R*)-1,2-bis(boranato(*i*-propyl)benzylphosphino)ethane: White crystals, (5%

EtOAc/Hexanes) $R_f=0.56$; $[\alpha]_D^{23}=-18.1$ (c , 1.0, CHCl_3); ^1H NMR (300 MHz, CDCl_3): δ 4.48(d, $J=354.8$, 2H), 1.84-2.19 (m, 4H), 1.18-1.32 (m, 14H), 0.43 (br. d, $J=92.59$, 6H); ^{13}C NMR (75 MHz, CDCl_3): 129.9, 128.9, 128.6, 128.5, 29.4 (d, $J=28.69$), 22.8 (d, $J=33.0$), 14.8 (d, $J=30.0$); 14.4 (s); ^{31}P NMR (121.4 MHz, CDCl_3): δ 29.4 (m).

6.3 Synthesis of the hydrovinylation catalysts

A 10 mL schlenk flask equipped with a stir bar was charged with **15** and then evacuated with argon. Freshly distilled morpholine was added to the reaction flask and heated at reflux for 3 hours. After removing morpholine via high vacuum, the reaction flask was placed into a nitrogen-filled drybox. The reaction flask then was charged with $\text{RuCl}_2[\text{COD}]_n$, removed from the drybox and filled with argon. Next, freshly distilled, degassed ethanol and Et_3N (15 equiv) were added in successive order. The reaction was then heated at reflux for 14-16 h. After which ethanol was removed via high vacuum. To remove triethylamine hydrochloride salt from the product, toluene was added to the

flask. After stirring for 30 minutes, the product was syringed filtered into another flask and the solvent was concentrated to give an orange/brown solid.

Product isolated from attempted synthesis of

(*R,R*)-1,2-bis((*tert*-butyl)benzylphosphino)ethane (CO)(Cl)RuH (13): ^1H NMR (300 MHz, CDCl_3): δ 6.82-7.72 (m, 10H), 3.54-3.86 (m, 4H), 1.51-1.39 (m, 4H), 0.96-1.56 (m, 18H), -10.19 (d, $J=36.8$, Ru-H) ^{13}C NMR (75 MHz, CDCl_3): 131.2-129.4 (m), 128.8, 128.6-127.8 (m), 127.2-126.1 (m), 42.8 (d, 63.40), 28.6-26.0 (m), 24.1, 13.7 (d, $J = 21.1$) ^{31}P NMR (121.4 MHz, CDCl_3): 145.7 (d, $J = 25.8$), 132.5-131.5 (m), 119.4 (d, $J = 25.7$), 118.9 (d, $J = 11.80$), 117.1 (d, $J = 18.5$), 109.5 (d, $J = 11.3$), 93.3 (d, $J = 7.2$), 91.6 (d, $J = 10.9$), 83.2 (d, $J = 8.6$), 81.4 (s); IR (cm^{-1} , film on NaCl): 2957, 1960, 1914, 1600, 1453.

Product isolated from attempted synthesis of

(*R,R*)-1,2-bis((cyclohexyl)cyclohexylphosphino)ethane (CO)(Cl)RuH (21): ^1H NMR (300 MHz, CDCl_3): δ 0.73-2.77 (m, 48H), -15.01 (dd, $J=10.0,27.1$, Ru-H) ^{13}C NMR (75 MHz, CDCl_3): 38.7-34.7 (m), 30.3-26.8 (m), 26.3, 25.7, 25.5 (d, $J = 18.5$); ^{31}P NMR (121.4 MHz, CDCl_3): 112.2 (d, $J = 28.6$), 109.9 (d, $J = 25.62$), 108.9 (d, $J = 13.5$), 103.2 (d, $J = 12.0$), 94.2 (s), 91.7-91.6 (m), 79.3 (s), 48.3-48.1 (m), 46.9 (d, $J = 4.2$), 46.7 (d, $J = 3.8$); IR (cm^{-1} , film on NaCl): 2926, 2851, 2046, 1952, 1447.

Product isolated from attempted synthesis of

(*R,R*)-1,2-bis((methyl)cyclohexylphosphino)ethane (CO)(Cl)RuH (22): ^1H NMR (300 MHz, CDCl_3): δ 0.98-2.76 (m, 32H), -21.27 (t, $J=19.7$, Ru-H) ^{13}C NMR (75 MHz, CDCl_3): 41.9 (d, $J = 23.1$), 39.5-34.6 (m), 25.6, 25.5 (d, $J = 28.9$), 15.2 (d, $J = 55.9$) ^{31}P

NMR (121.4 MHz, CDCl₃): 92.1 (d, $J = 15.9$), 88.3-87.7 (m), 84.47 (t, $J = 18.2, 18.2$), 81.8-81.2 (m), 78.8 (d, $J = 15.9$), 77.6 (d, $J = 20.0$), 71.19, 69.1, 65.4-65.0 (m), 64.0 (t, $J = 21.4, 20.9$) IR (cm⁻¹, film on NaCl): 2923, 2851, 1930, 1564, 1447.

Product isolated from attempted synthesis of

(*R,R*)-1,2-bis((cyclohexyl)benzylphosphino)ethane (CO)(Cl)RuH (23): ¹H NMR (300 MHz, CDCl₃): δ 7.01-7.64 (m, 10H), 3.02-4.11 (m, 8H), 0.70-1.62 (m, 24H), -14.03 (d, $J = 21.7$, Ru-H) ¹³C NMR (75 MHz, CDCl₃): 129.8, 128.9, 128.6, 128.5, 128.2, 126.7, 29.3 (d, $J = 30.3$), 28.2 (d, $J = 39.9$), 27.6 (d, $J = 14.3$), 26.8 (d, $J = 60.7$ Hz), 24.7 (d, $J = 13.6$) ³¹P NMR (121.4 MHz, CDCl₃): 145.8 (d, $J = 27.0$), 131.8 (d, $J = 20.3$), 119.5 (d, $J = 25.5$), 118.9 (d, $J = 11.2$), 117.1 (d, $J = 19.5$), 109.5 (d, $J = 12.1$), 93.2 (d, $J = 8.1$), 92.5 (d, $J = 11.3$), 91.5 (d, $J = 10.3$), 82.0 (d, $J = 33.6$), 81.3 (s) IR (cm⁻¹, film on NaCl): 2957, 1960, 1604, 1450.

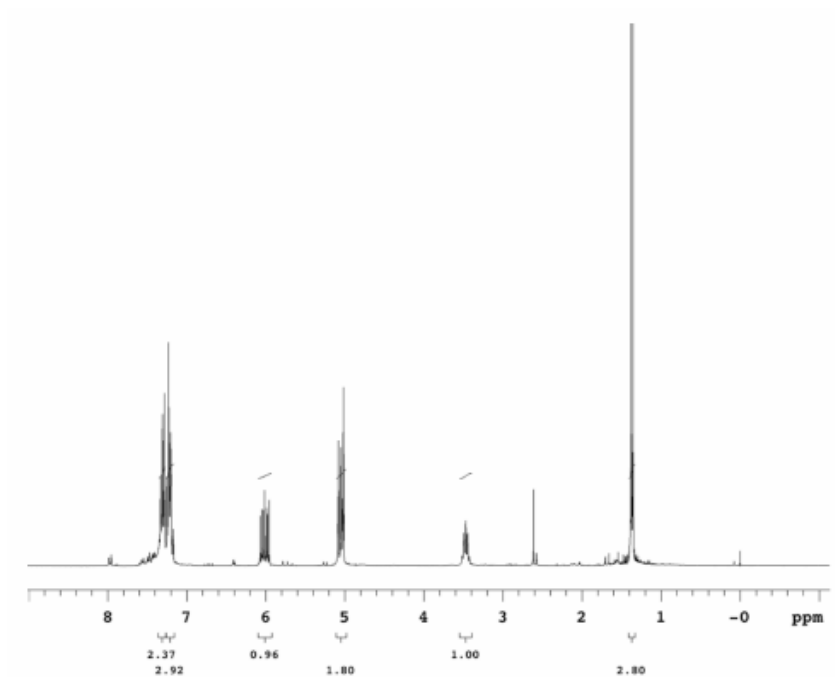
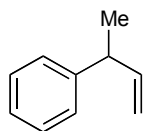
REFERENCES

1. RajanBabu, T. V. *Chem. Rev.* **2003**, *103*, 2845-2860.
2. RajanBabu, T. V.; Nomura, N.; Jin, J.; Nandi, M.; Park, H.; Sun, X. *J. Org. Chem.* **2003**, *68*, 8431-8446.
3. Wilke, G.; Bogdanovic, B.; Hardt, P.; Heimbach, P.; Keim, W.; Kroner, M.; Oberkirch, W.; Tanaka, K.; Steinrucke, E.; Walter, D.; Zimmermann, H. *Angew. Chem. Int. Ed.* **1966**, *5*, 151-164.
4. Wilhelm, K. *Angew. Chem. Int. Ed.* **1990**, *29*, 235-244.
5. Alderson, T.; Jenner, E. L.; Lindsey, R. V. *J. Am. Chem. Soc.* **1965**, *87*, 5638-5645.
6. Kawata, N.; Maruya, K.; Mizoroki, T.; Ozaki, A. *Bull. Chem. Soc. Jpn.* **1971**, *44*, 3217.
7. Kawata, N.; Maruya, K.; Mizoroki, T.; Ozaki, A. *Bull. Chem. Soc. Jpn.* **1974**, *47*, 413-416.
8. Barlow, M. G.; Bryant, M. J.; Haszeldine, R. N.; Mackie, A. G. *J. Organomet. Chem.* **1970**, *21*, 215-226.
9. Kawamoto, K.; Tatani, A.; Imanaka, T.; Teranish.S *Bull. Chem. Soc. Jpn.* **1971**, *44*, 1239.
10. Nozima, H.; Kawata, N.; Nakamura, Y.; Maruya, K.; Mizoroki, T.; Ozaki, A. *Chem. Lett.* **1973**, 1163-1164.
11. Pillai, S. M.; Tembe, G. L.; Ravindranathan, M. *J. Mol. Catal.* **1993**, *84*, 77-86.
12. Umezaki, H.; Fujiwara, Y.; Sawara, K.; Teranish.S *Bull. Chem. Soc. Jpn.* **1973**, *46*, 2230-2231.
13. Hilt, G.; Luers, S. *Synthesis* **2002**, 609-618.
14. Bogdanovic, B.; H., B.; Meister, B.; Pauling, H.; Wilke, G. *Angew. Chem. Int. Ed.* **1972**, *11*, 1023-1024.
15. Bogdanovic, B.; H., B.; Meister, B.; Pauling, H.; Wilke, G.; Losler, A. *Angew. Chem. Int. Ed.* **1973**, *12*, 954-964.
16. Ceder, R.; Muller, G.; Ordinas, J. I. *J. Mol. Catal.* **1994**, *92*, 127-139.

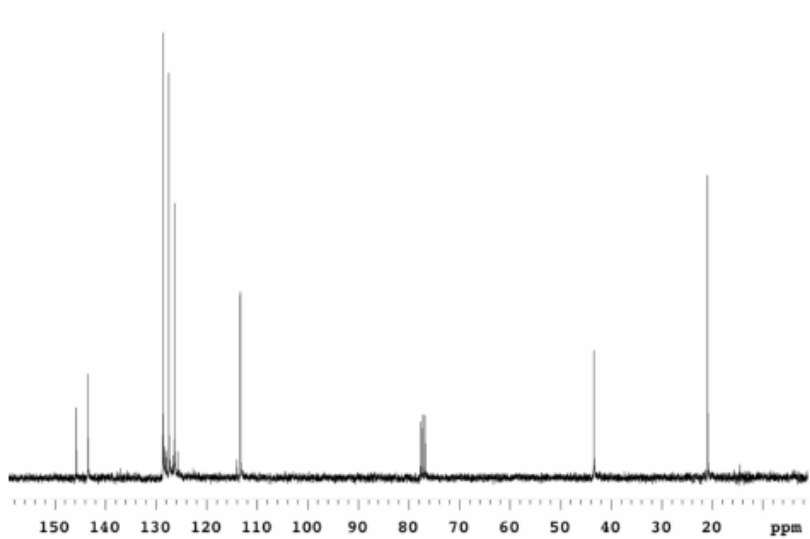
17. Muller, G.; Ordinas, J. I. *J. Mol. Catal., A: Chem.* **1997**, *125*, 97-108.
18. Nomura, N.; Jin, J.; Park, H.; RajanBabu, T. V. *J. Am. Chem. Soc.* **1998**, *120*, 459-460.
19. Uozumi, Y.; Tanahashi, A.; Lee, S. Y.; Hayashi, T. *J. Org. Chem.* **1993**, *58*, 1945-1948.
20. Britovsek, G. J. P.; Keim, W.; Mecking, S.; Sainz, D.; Wagner, T. *J. Chem. Soc., Chem. Comm.* **1993**, 1632-1634.
21. Feringa, B. L. *Acc. Chem. Res.* **2000**, *33*, 346-353.
22. Smith, C. R.; RajanBabu, T. V. *Org. Lett.* **2008**, *10*, 1657-1659.
23. Shi, W.-J.; Xie, J.-H.; Zhou, Q.-L. *Tetrahedron: Asymmetry* **2005**, *16*, 705-710.
24. Shi, W. J.; Zhang, Q.; Xie, J. H.; Zhu, S. F.; Hou, G. H.; Zhou, Q. L. *J. Am. Chem. Soc.* **2006**, *128*, 2780-2781.
25. Zhang, A.; RajanBabu, T. V. *J. Am. Chem. Soc.* **2006**, *128*, 5620-5621.
26. Pillai, S. M.; Ravindranathan, M.; Sivaram, S. *Chem. Rev.* **1986**, *86*, 353-399.
27. Yi, C. S.; Lee, D. W.; Chen, Y. *Organometallics* **1999**, *18*, 2043-2045.
28. Yi, C. S. *Synlett* **1999**, 281-287.
29. Yi, C. S.; He, Z.; Lee, D. W. *Organometallics* **2001**, *20*, 802-804.
30. Kawano, H.; Ikariya, T.; Ishii, Y.; Kodama, T.; Saburi, M.; Yoshikawa, S.; Uchida, Y.; Akutagawa, S. *Bull. Chem. Soc. Jpn.* **1992**, *65*, 1595-1602.
31. Ahmad, N.; Levison, J. J.; Robinson, S. D.; Uttley, M. F. *Inorg. Synth.* **1974**, *15*, 45.
32. Park, Y. J.; Huh, S.; Youm, K. T.; Jun, Y. J.; Jun, M. J. *Bull. Kor. Chem. Soc.* **2000**, *21*, 939-942.
33. Yamanoi, Y.; Imamoto, T. *J. Org. Chem.* **1999**, *64*, 2988-2989.
34. Imamoto, T.; Watanabe, J.; Wada, Y.; Masuda, H.; Yamada, H.; Tsuruta, H.; Matsukawa, S.; Yamaguchi, K. *J. Am. Chem. Soc.* **1998**, *120*, 1635-1636.

35. Schroder, M.; Nozaki, K.; Hiyama, T. *Bull. Chem. Soc. Jpn.* **2004**, *77*, 1931-1932.
36. Landaeta, V. R.; Peruzzini, M.; Herrera, V.; Bianchini, C.; Sanchez-Delgado, R. A.; Goeta, A. E.; Zanobini, F. *J. Organometallic Chem.* **2006**, *691*, 1039-1050.
37. Empsall, H. D.; Hyde, E. M.; Mentzer, E.; Shaw, B. L.; Uttley, M. F. *J. Chem. Soc. Dalton Trans.* **1976**, 2069-2074.
38. Tolman, C. A. *Chem. Rev.* **1977**, *77*, 313-348.
39. Crépy, K. V. L.; Imamoto, T. *Tetrahedron Lett.* **2002**, *43*, 7735-7737.
40. Crépy, K. V. L.; Imamoto, T. In *New Aspects in Phosphorus Chemistry III*, Springer Berlin, Heidelberg, 2003, p 111-141.
41. Bothe, U.; Rudbeck, H. C.; Tanner, D.; Johannsen, M. *J. Chem. Soc. Perkin Trans. I* **2001**, 3305-3311.
42. He, J.; Muller, M.; Hertweck, C. *J. Am. Chem. Soc.* **2004**, *126*, 16742-16743.
43. Fairlamb, I. J. S.; McGlacken, G. P.; Weissberger, F. *Chemical Communications* **2006**, 988-990.
44. Majik, M. S.; Parameswaran, P. S.; Tilve, S. G. *J. Org. Chem.* **2009**, *74*, 3591-3594.
45. Moloney, M. G. *Nat. Prod. Rep.* **2002**, *19*, 597-616.
46. Mohmmad, A. S., R; Keller J.; St. Clair, D.; Markesbery, W.; Butterfield, D. *J. Neurochem.* **2006**, *96*, 1322-1335.
47. Sperk, G. *Prog. Neurobiol.* **1994**, *42*, 1-32.
48. Nagata, K.; Matsukawa, S.; Imamoto, T. *J. Org. Chem.* **2000**, *65*, 4185-4188.
49. Fassina, V.; Ramminger, C.; Seferin, M.; Monteiro, A. L. *Tetrahedron* **2000**, *56*, 7403-7409.
50. Fouquet, E.; Pereyre, M.; Rodriguez, A. L. *J. Org. Chem.* **1997**, *62*, 5242-5243.
51. Yamamoto, Y.; Takada, S.; Miyaura, N. *Chem. Lett.* **2006**, *35*, 704-705.

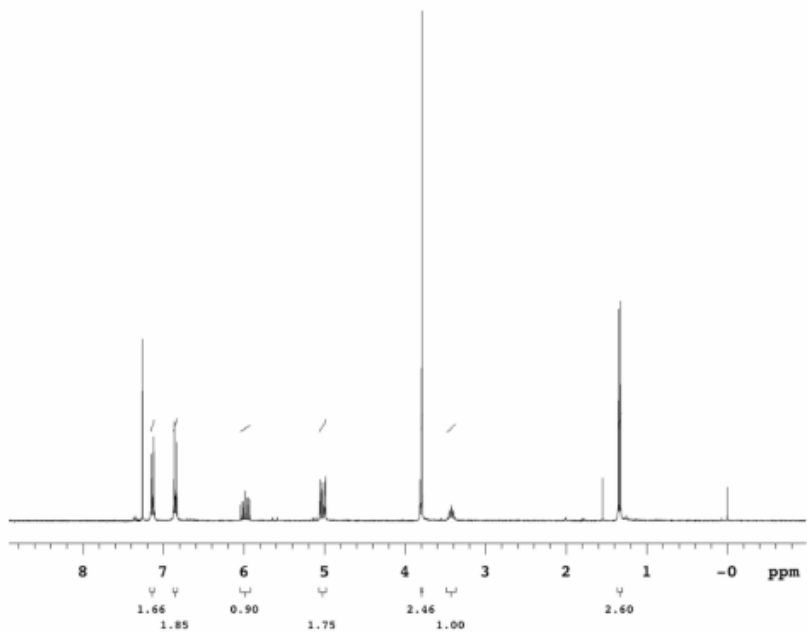
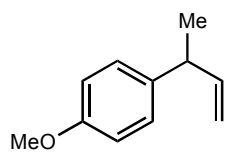
APPENDIX A
NMR SPECTRA



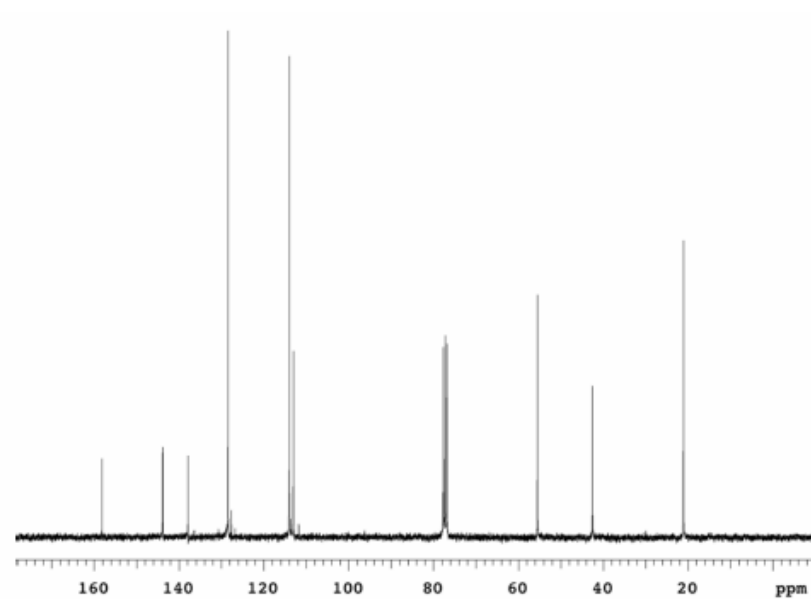
^1H (CDCl₃, 300 MHz)



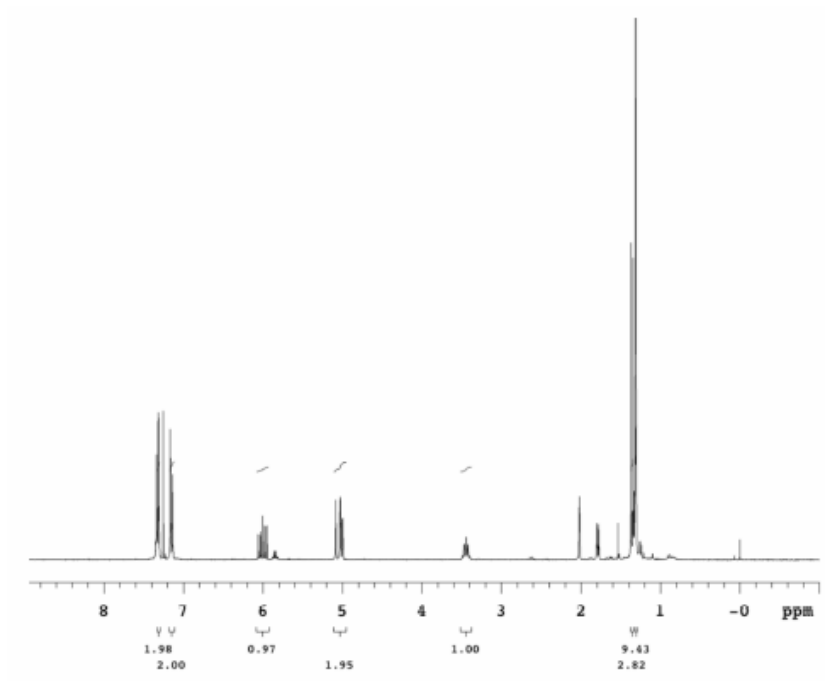
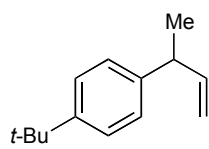
^{13}C (CDCl₃, 75 MHz)



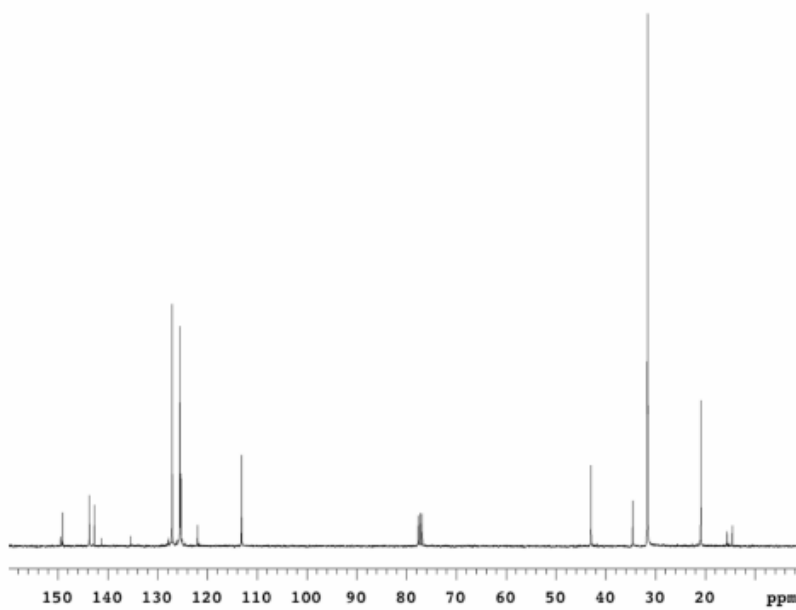
^1H (CDCl₃, 300 MHz)



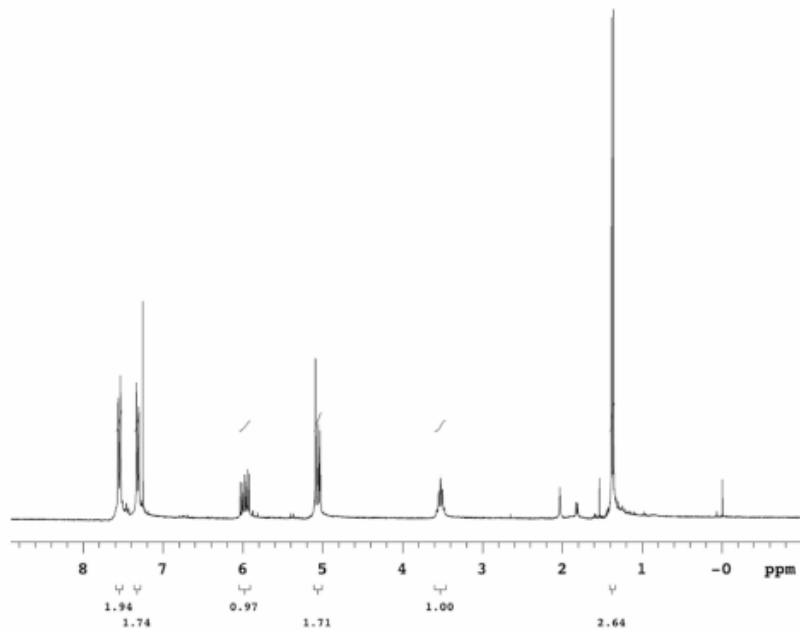
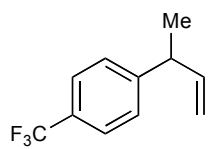
^{13}C (CDCl₃, 75 MHz)



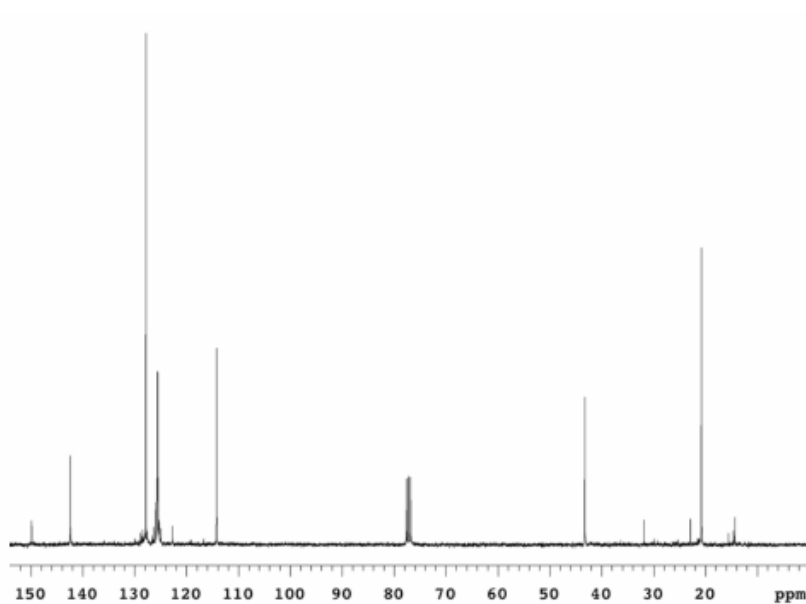
¹H (CDCl₃, 300 MHz)



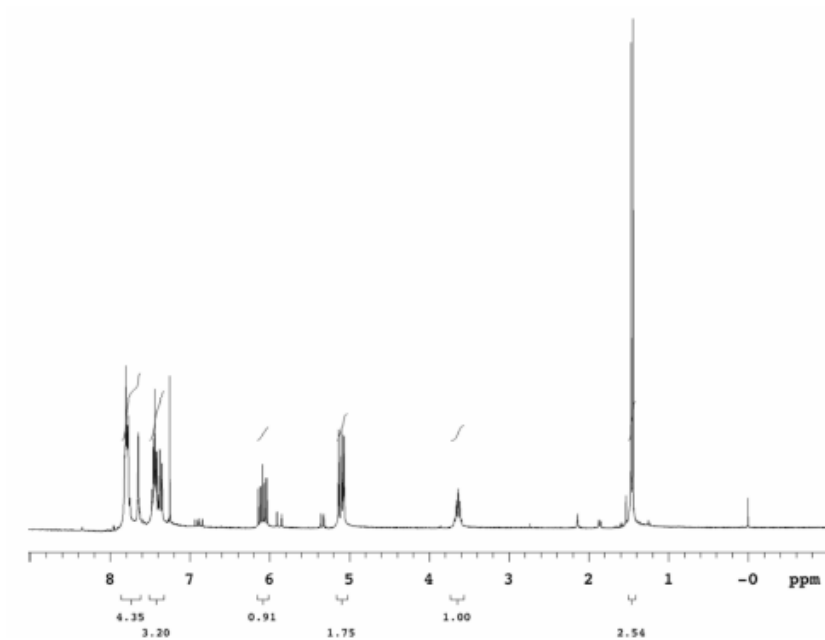
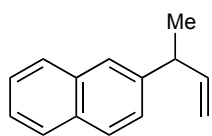
¹³C (CDCl₃, 75 MHz)



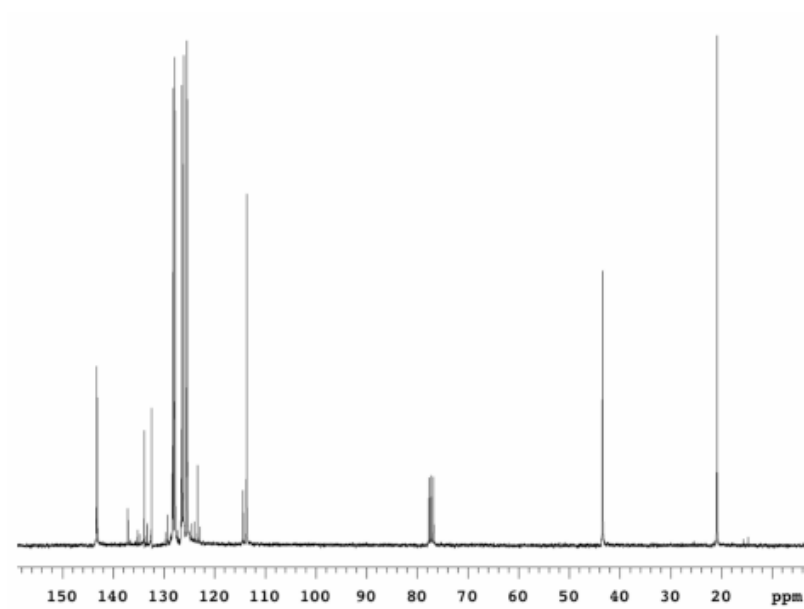
¹H (CDCl₃, 300 MHz)



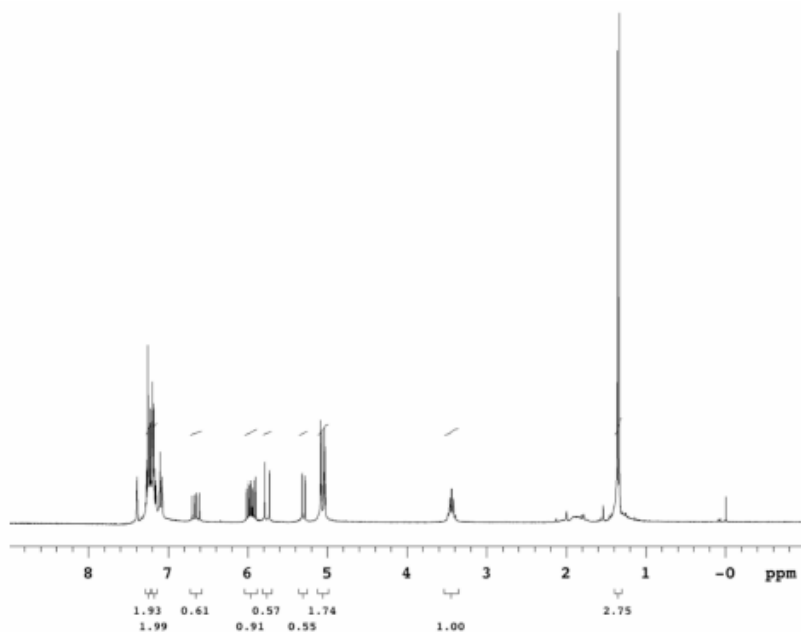
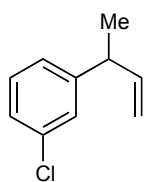
¹³C (CDCl₃, 75 MHz)



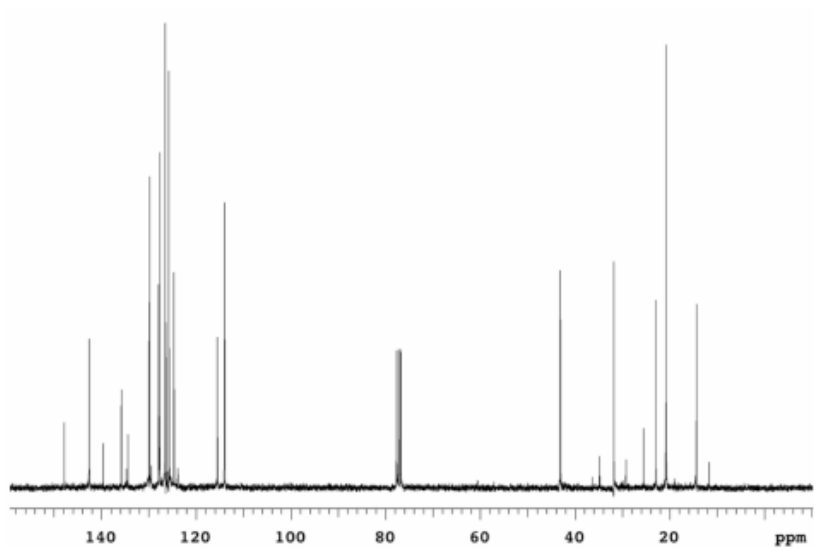
^1H (CDCl_3 , 300 MHz)



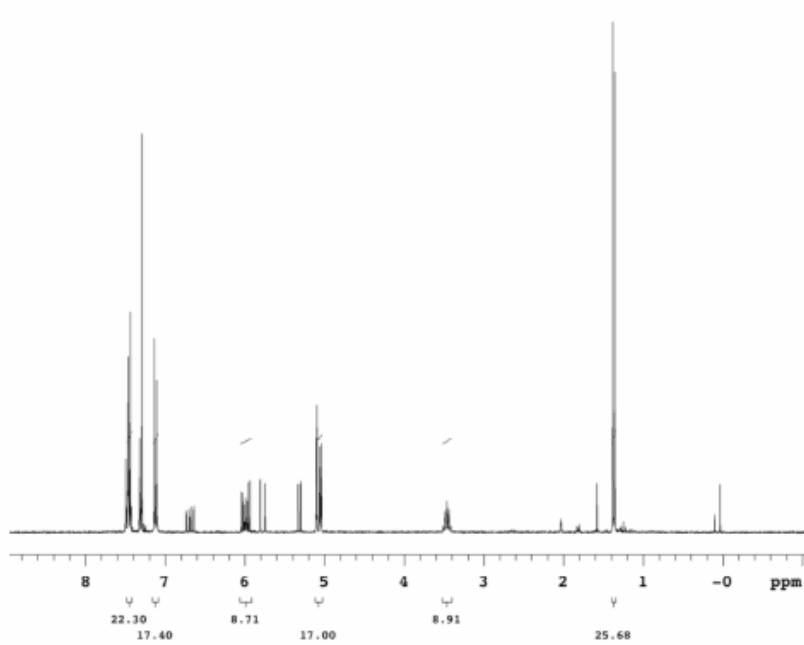
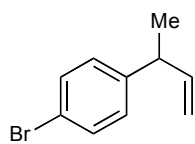
^{13}C (CDCl_3 , 75 MHz)



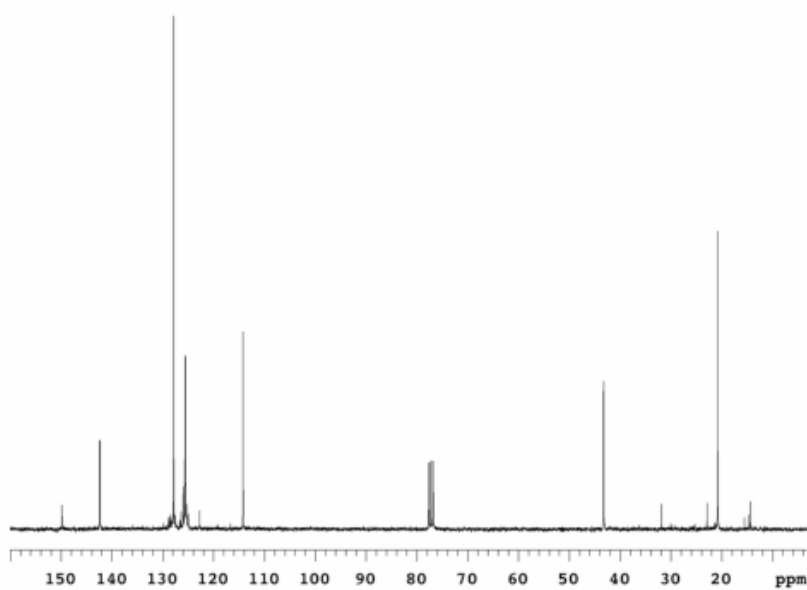
^1H (CDCl_3 , 300 MHz)



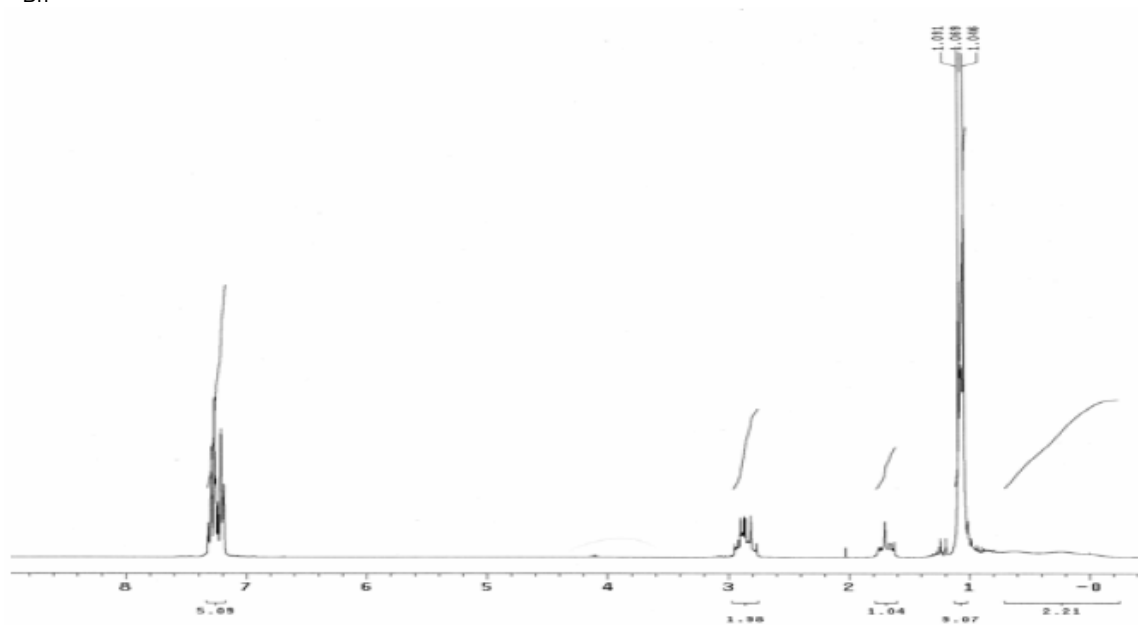
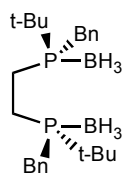
^{13}C (CDCl_3 , 75 MHz)



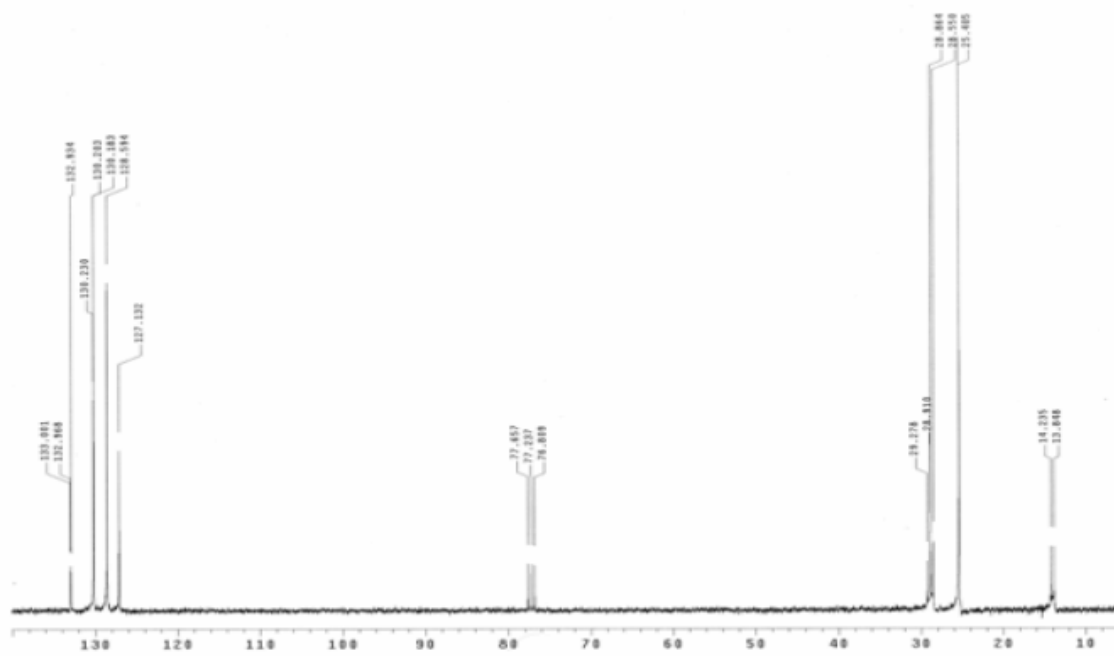
^1H (CDCl₃, 300 MHz)



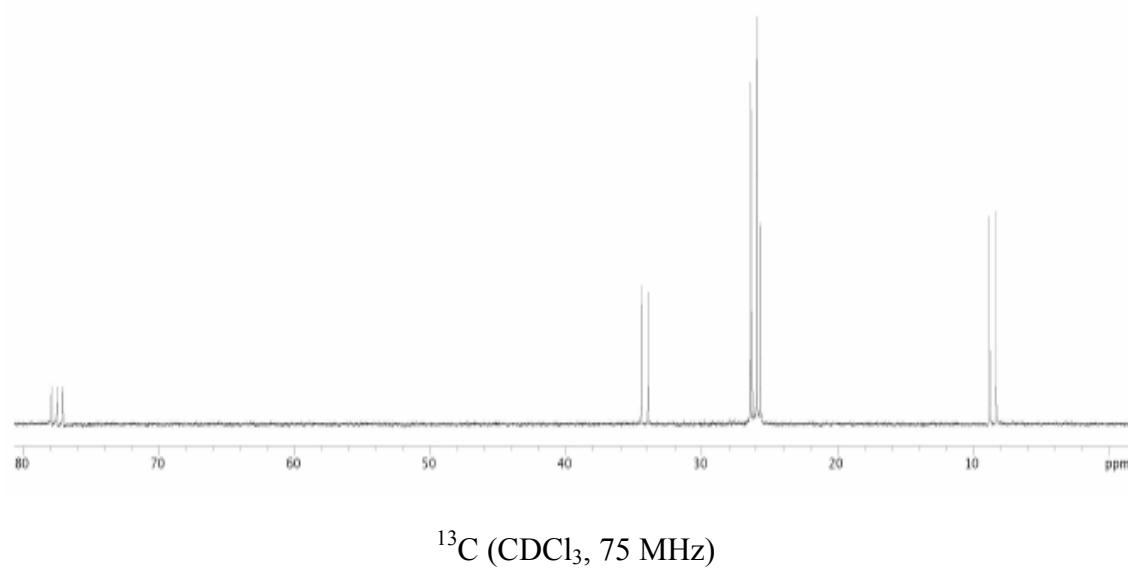
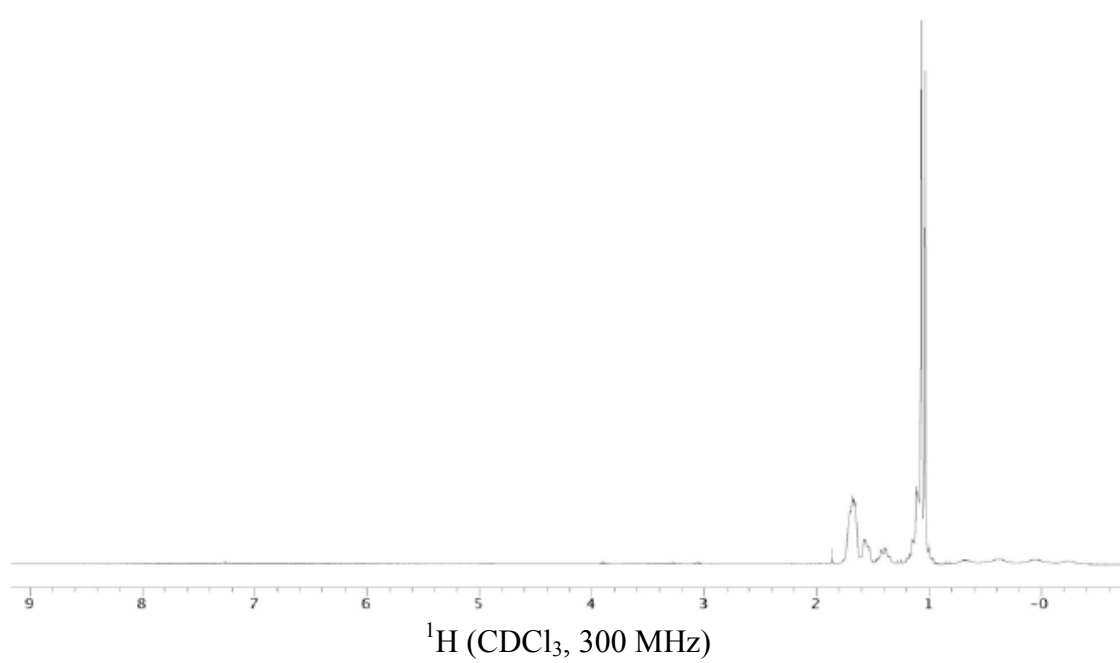
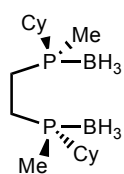
^{13}C (CDCl₃, 75 MHz)

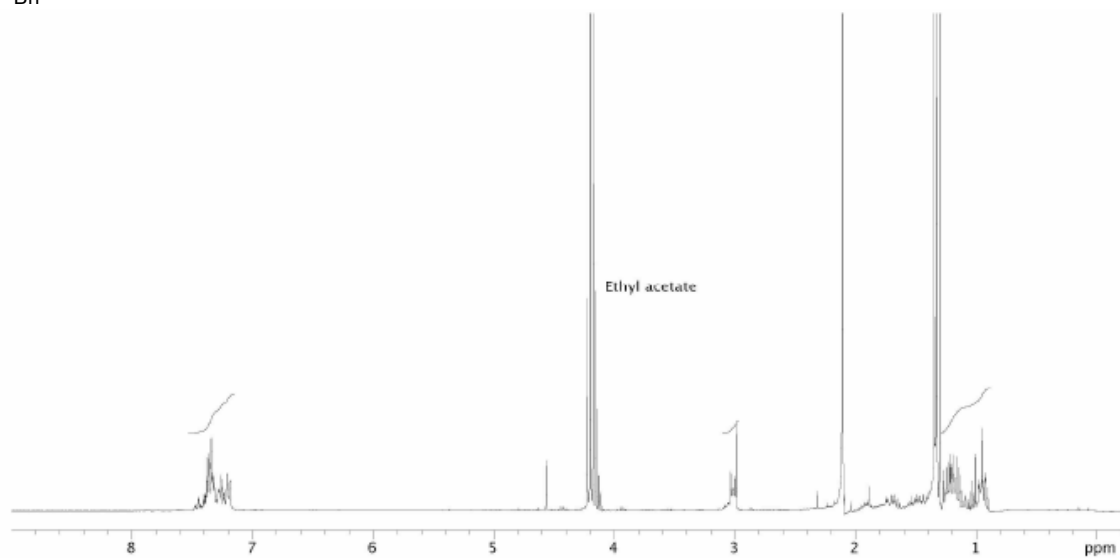
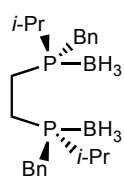


¹H (CDCl₃, 300 MHz)

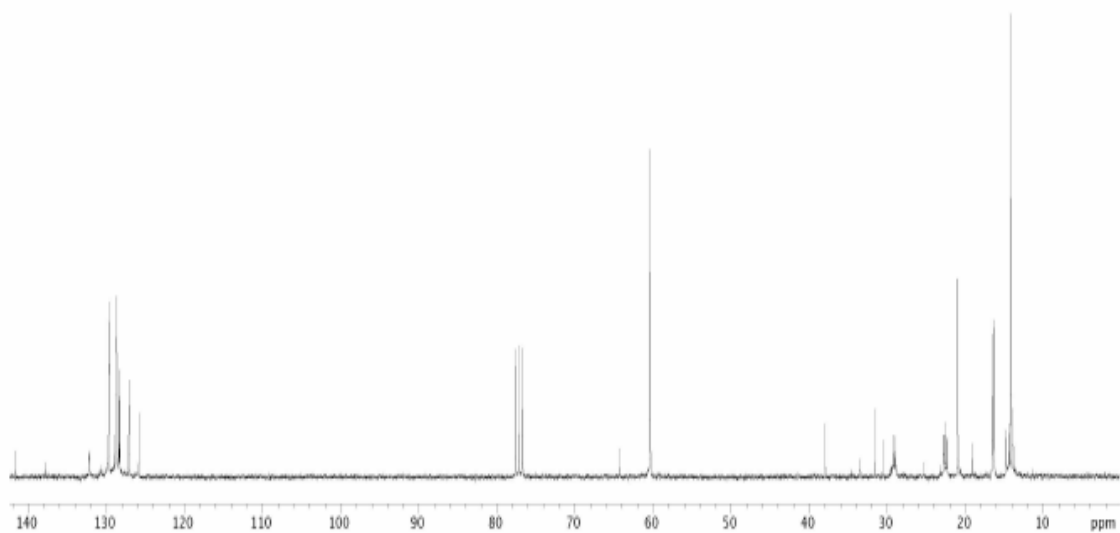


¹³C (CDCl₃, 75 MHz)

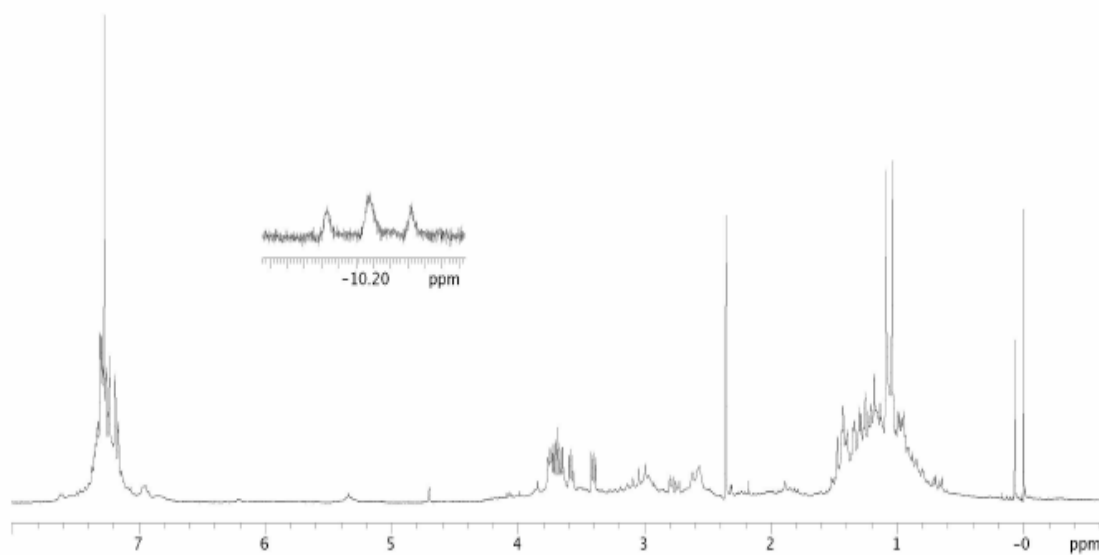
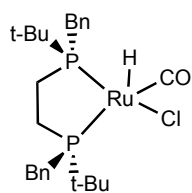




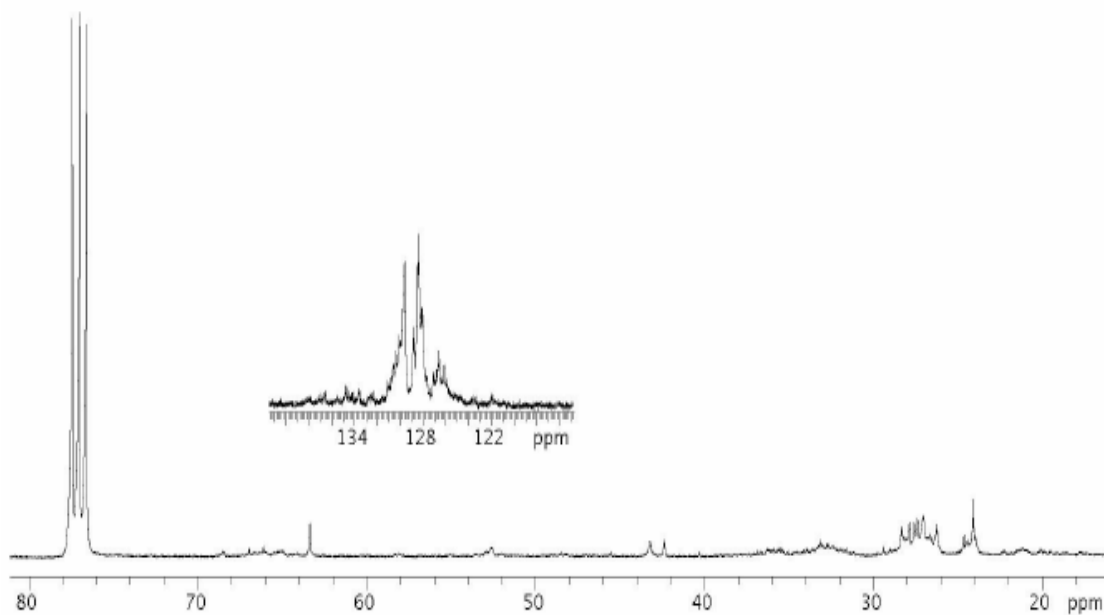
¹H (CDCl₃, 300 MHz)



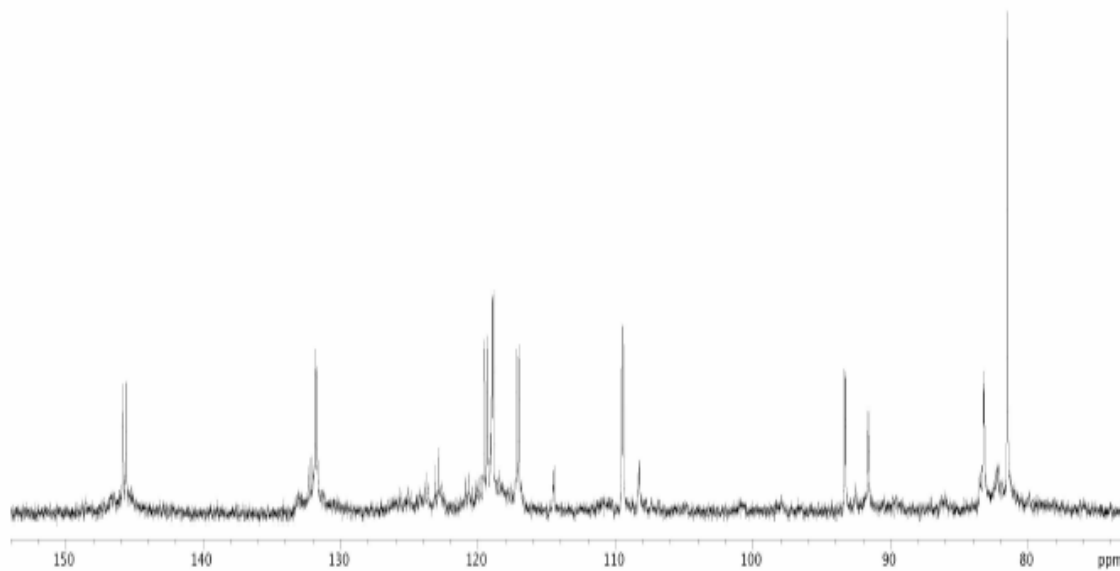
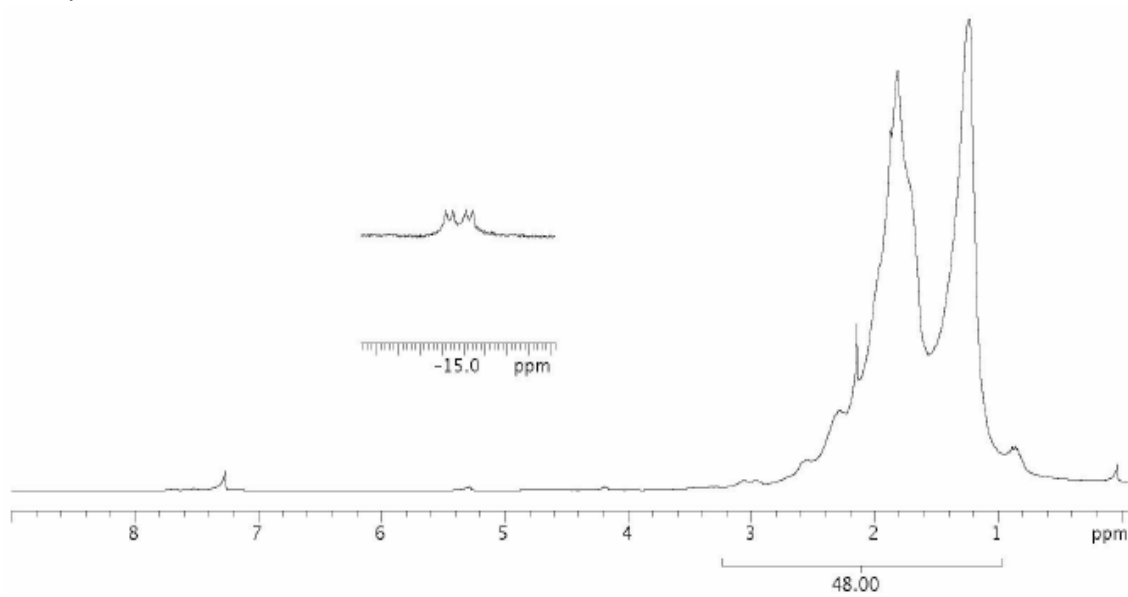
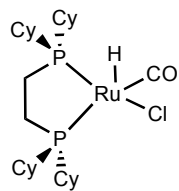
¹³C (CDCl₃, 75 MHz)

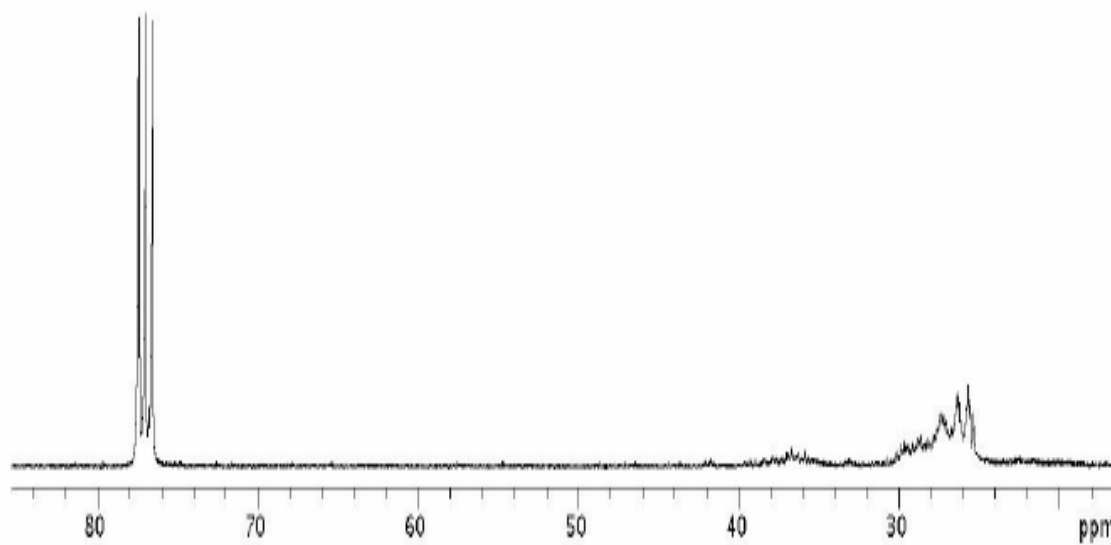
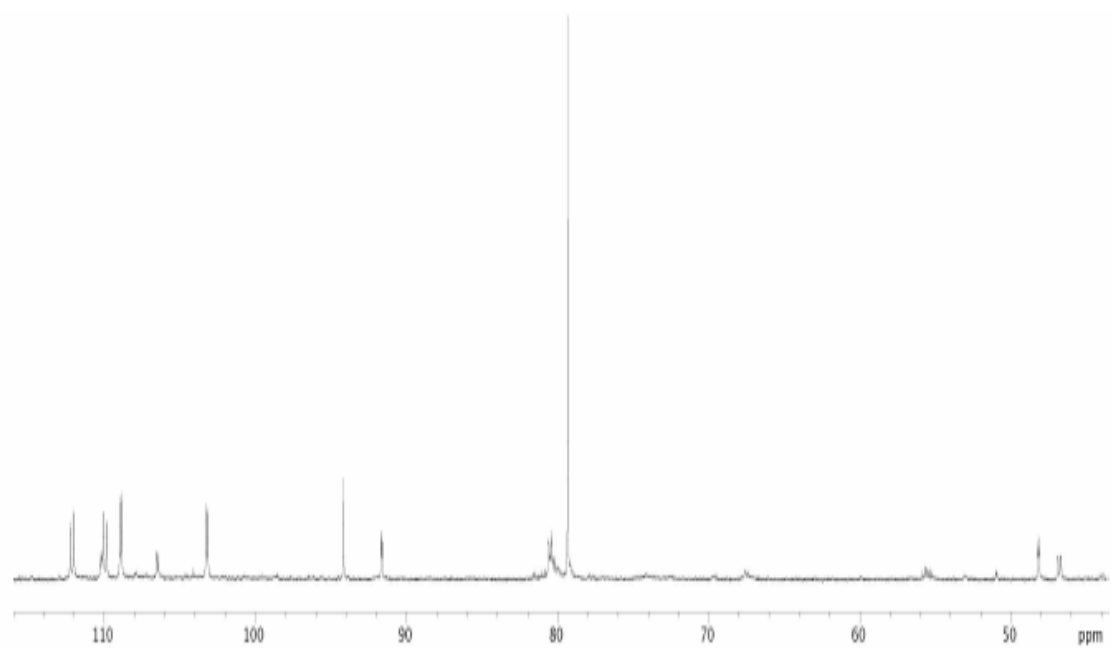


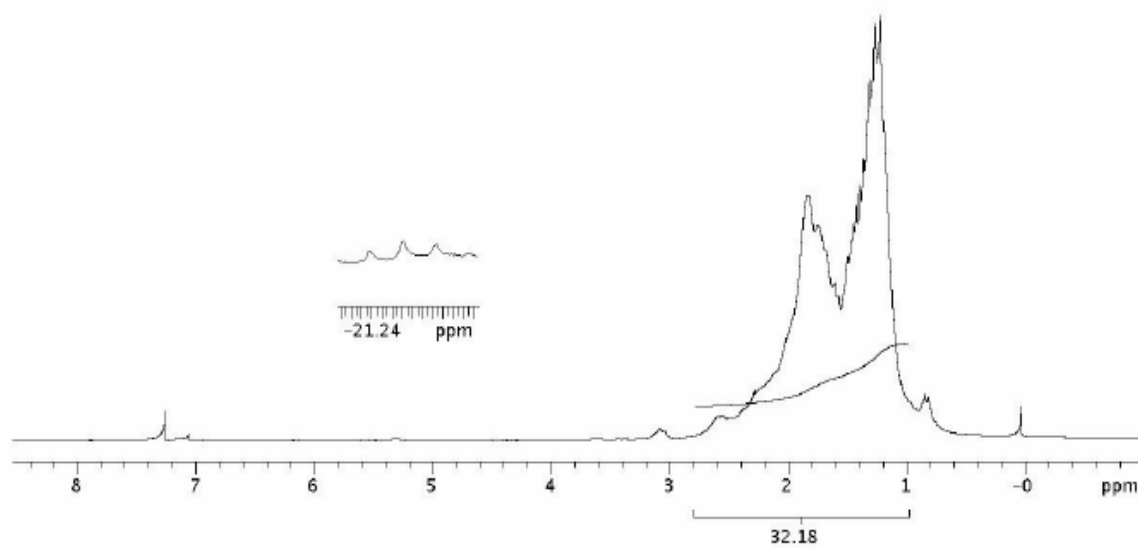
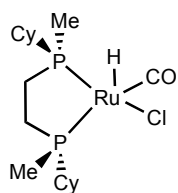
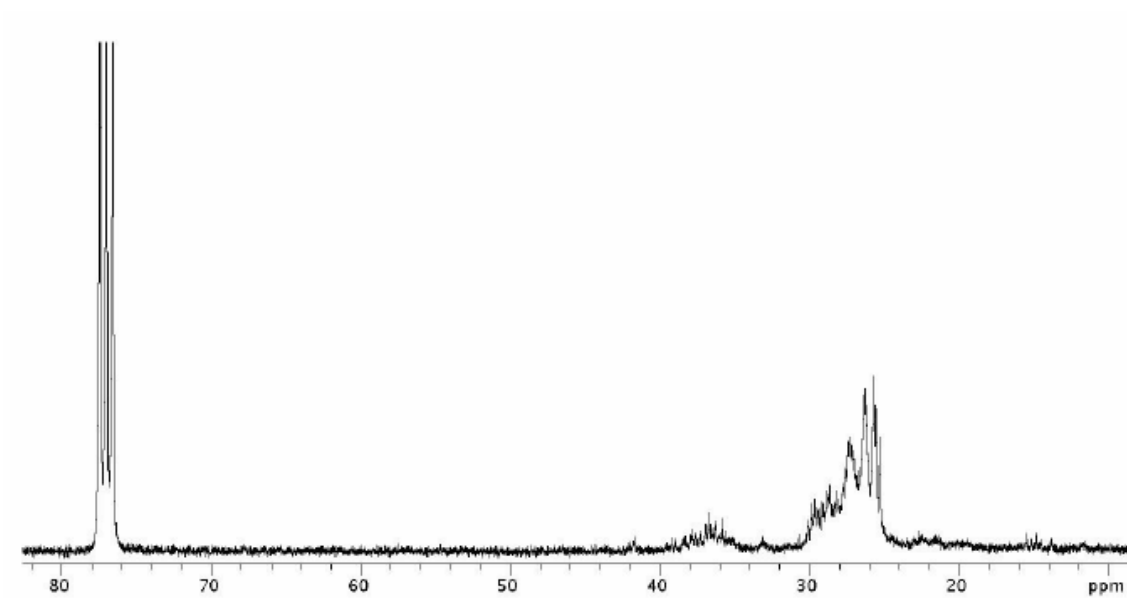
^1H (CDCl_3 , 300 MHz)

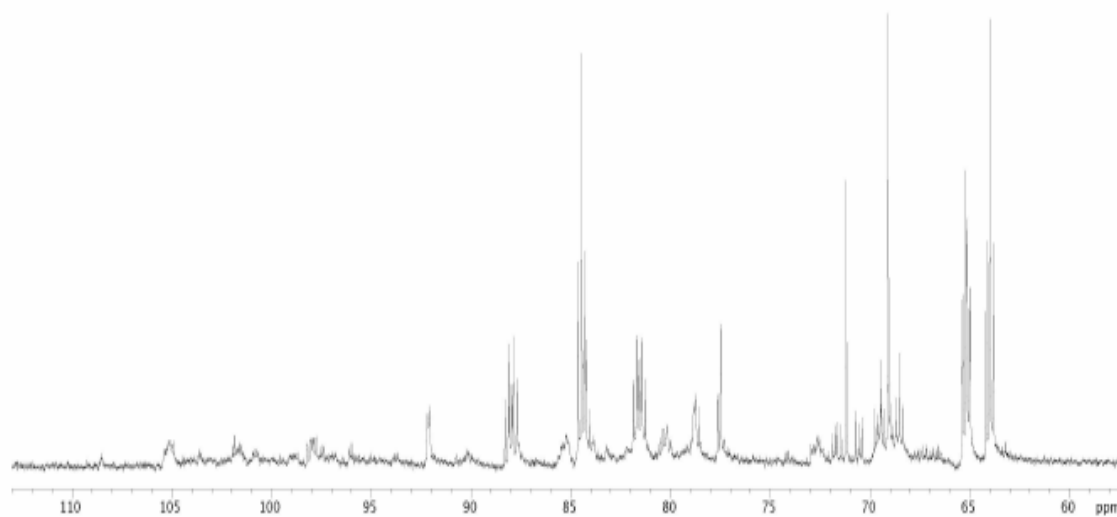
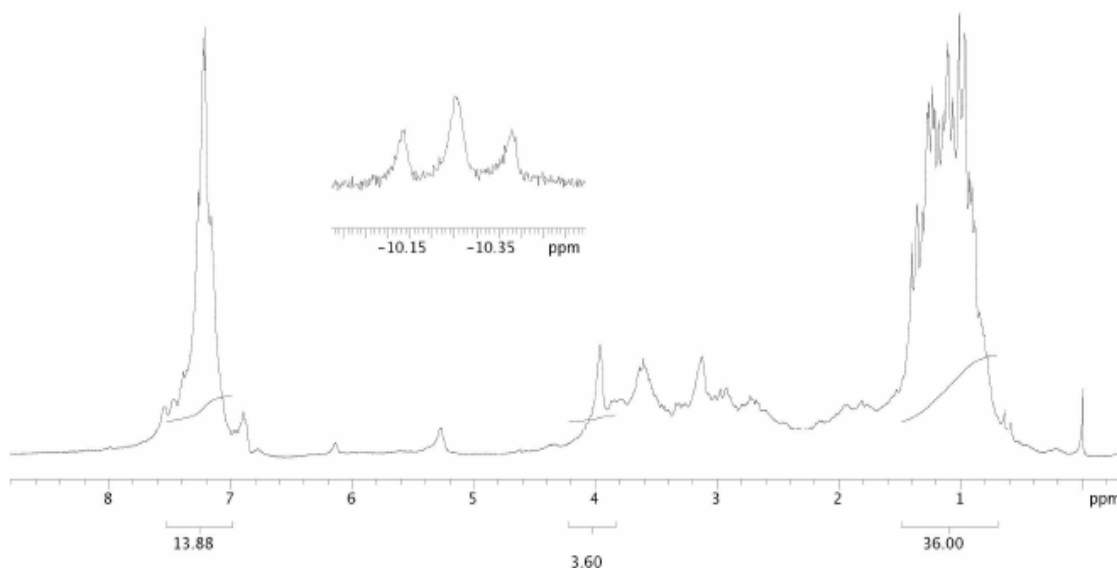
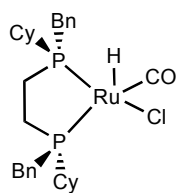


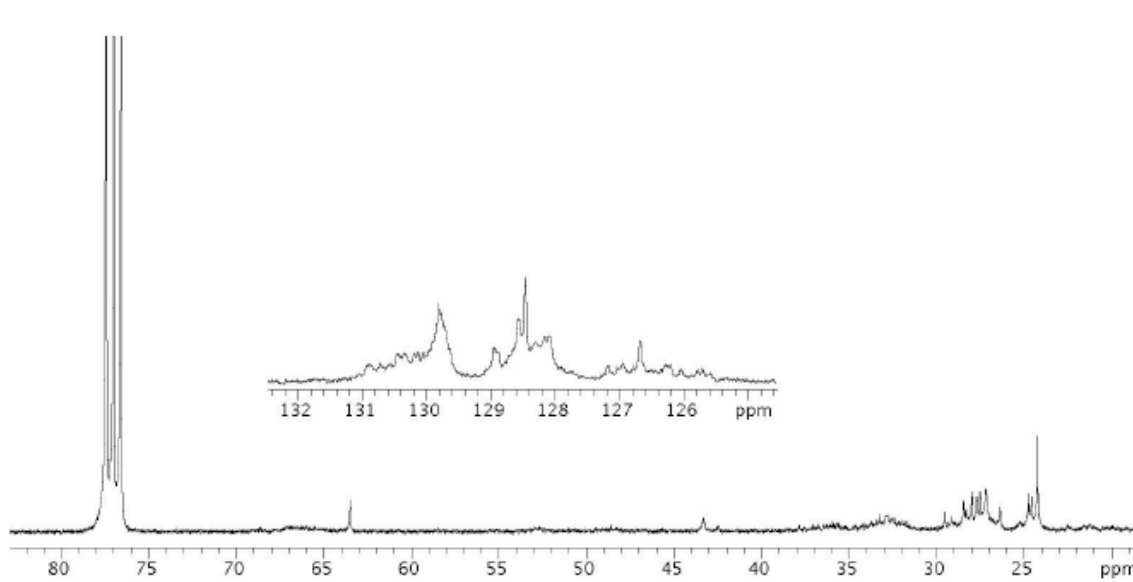
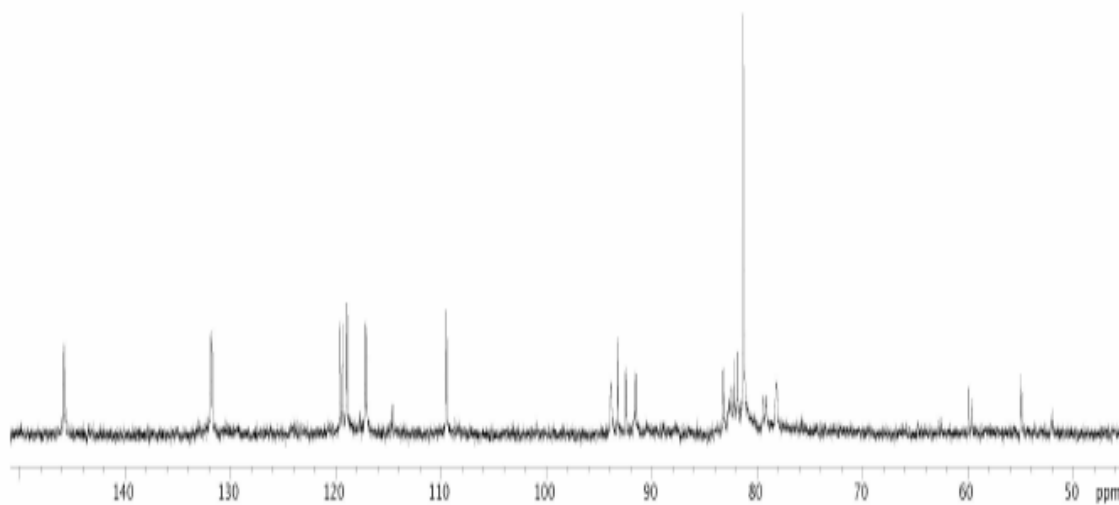
^{13}C (CDCl_3 , 75 MHz)

 ^{31}P (CDCl_3 , 121 MHz) ^1H (CDCl_3 , 300 MHz)

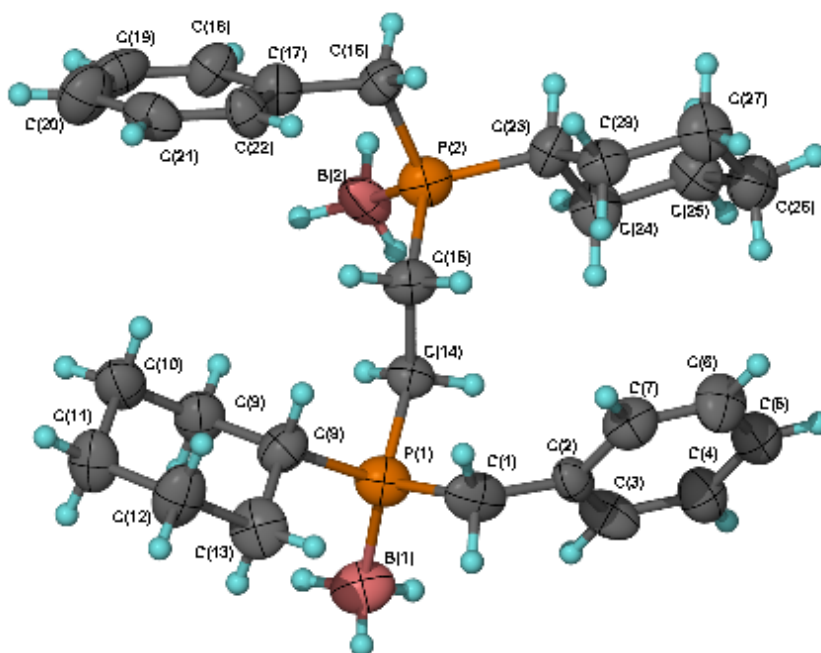
 ^{13}C (CDCl₃, 75 MHz) ^{31}P (CDCl₃, 121 MHz)

 ^1H (CDCl_3 , 300 MHz) ^{13}C (CDCl_3 , 75 MHz)

 ^{31}P (CDCl_3 , 121 MHz) ^1H (CDCl_3 , 300 MHz)

 ^{13}C (CDCl_3 , 75 MHz) ^{31}P (CDCl_3 , 121 MHz)

APPENDIX B
CRYSTAL STRUCTURE OF (*R,R*)-1,2-
BIS(BORANATO(CYCLOHEXYL)BENZYLPHOSPHINO)ETHANE



Notes :

Chiral Centers are both *R*.

Absolute Configuration was determined.

Flack Parameter = 0.05(3)

Table 1. Crystal data and structure refinement for bc26.

Identification code	bc26	
Empirical formula	C ₂₈ H ₄₆ B ₂ P ₂	
Formula weight	466.21	
Temperature	110(2) K	
Wavelength	1.54184 Å	
Crystal system	Monoclinic	
Space group	P2(1)	
Unit cell dimensions	a = 6.4223(15) Å	∠ = 90°.
	b = 18.293(4) Å	∠ = 104.751(18)°.
	c = 12.360(3) Å	∠ = 90°.
Volume	1404.3(6) Å ³	
Z	2	
Density (calculated)	1.103 Mg/m ³	
Absorption coefficient	1.480 mm ⁻¹	
F(000)	508	
Crystal size	0.13 x 0.05 x 0.01 mm ³	
Theta range for data collection	4.83 to 59.99°.	
Index ranges	-7 ≤ h ≤ 7, -20 ≤ k ≤ 20, -13 ≤ l ≤ 13	
Reflections collected	18099	
Independent reflections	3900 [R(int) = 0.1522]	
Completeness to theta = 59.99°	97.7 %	
Absorption correction	Semi-empirical from equivalents	
Max. and min. transmission	0.9854 and 0.8309	
Refinement method	Full-matrix least-squares on F ²	
Data / restraints / parameters	3900 / 1 / 293	
Goodness-of-fit on F ²	1.002	
Final R indices [I > 2σ(I)]	R1 = 0.0626, wR2 = 0.0986	
R indices (all data)	R1 = 0.1510, wR2 = 0.1179	
Absolute structure parameter	0.05(3)	
Extinction coefficient	0.0101(5)	
Largest diff. peak and hole	0.259 and -0.266 e.Å ⁻³	

Table 2. Atomic coordinates ($\times 10^4$) and equivalent isotropic displacement parameters ($\text{\AA}^2 \times 10^3$) for bc26. $U(\text{eq})$ is defined as one third of the trace of the orthogonalized U^{ij} tensor.

	x	y	z	$U(\text{eq})$
P(1)	8941(3)	-23(1)	6502(2)	55(1)
P(2)	6743(2)	2281(1)	5499(2)	53(1)
C(1)	10814(10)	-191(4)	5662(6)	60(2)
C(2)	9991(10)	-119(4)	4422(6)	44(2)
C(3)	8091(10)	-417(4)	3812(7)	58(2)
C(4)	7377(11)	-321(4)	2632(7)	59(2)
C(5)	8601(11)	94(4)	2096(6)	58(2)
C(6)	10516(11)	395(4)	2715(7)	61(2)
C(7)	11165(11)	293(4)	3851(7)	58(2)
C(8)	10723(10)	300(4)	7839(5)	52(2)
C(9)	9415(10)	587(4)	8623(6)	58(2)
C(10)	10945(10)	893(4)	9685(6)	60(2)
C(11)	12569(10)	315(4)	10246(6)	62(2)
C(12)	13830(10)	2(4)	9434(6)	68(2)
C(13)	12245(9)	-303(4)	8362(6)	63(2)
C(14)	7341(9)	776(3)	5908(5)	42(2)
C(15)	8537(9)	1512(3)	5971(6)	49(2)
C(16)	8314(9)	3089(3)	6113(6)	46(2)
C(17)	8887(10)	3092(4)	7384(6)	51(2)
C(18)	7318(10)	3282(4)	7944(7)	53(2)
C(19)	7847(11)	3311(4)	9096(8)	66(2)
C(20)	9934(12)	3166(4)	9735(7)	70(2)
C(21)	11450(10)	2957(4)	9142(7)	58(2)
C(22)	10924(10)	2931(4)	7985(6)	48(2)
C(23)	6386(9)	2441(3)	3981(5)	47(2)
C(24)	4615(9)	1973(4)	3296(6)	58(2)
C(25)	4252(9)	2173(4)	2059(6)	55(2)
C(26)	6289(10)	2083(4)	1654(6)	62(2)
C(27)	8118(9)	2507(4)	2381(6)	60(2)

C(28)	8475(8)	2329(4)	3621(6)	48(2)
B(1)	7100(12)	-843(4)	6618(8)	67(3)
B(2)	4101(10)	2165(4)	5913(7)	58(3)

Table 3. Bond lengths [\AA] and angles [$^\circ$] for bc26.

P(1)-C(1)	1.805(6)
P(1)-C(14)	1.829(6)
P(1)-C(8)	1.851(6)
P(1)-B(1)	1.938(7)
P(2)-C(15)	1.817(6)
P(2)-C(16)	1.840(6)
P(2)-C(23)	1.854(6)
P(2)-B(2)	1.905(6)
C(1)-C(2)	1.495(8)
C(1)-H(1D)	0.9900
C(1)-H(1E)	0.9900
C(2)-C(3)	1.374(8)
C(2)-C(7)	1.380(9)
C(3)-C(4)	1.424(8)
C(3)-H(3)	0.9500
C(4)-C(5)	1.378(8)
C(4)-H(4)	0.9500
C(5)-C(6)	1.386(8)
C(5)-H(5)	0.9500
C(6)-C(7)	1.372(9)
C(6)-H(6)	0.9500
C(7)-H(7)	0.9500
C(8)-C(13)	1.506(8)
C(8)-C(9)	1.528(8)
C(8)-H(8)	1.0000
C(9)-C(10)	1.532(8)
C(9)-H(9A)	0.9900
C(9)-H(9B)	0.9900
C(10)-C(11)	1.522(8)
C(10)-H(10A)	0.9900
C(10)-H(10B)	0.9900
C(11)-C(12)	1.551(8)

C(11)-H(11A)	0.9900
C(11)-H(11B)	0.9900
C(12)-C(13)	1.555(8)
C(12)-H(12A)	0.9900
C(12)-H(12B)	0.9900
C(13)-H(13A)	0.9900
C(13)-H(13B)	0.9900
C(14)-C(15)	1.542(7)
C(14)-H(14A)	0.9900
C(14)-H(14B)	0.9900
C(15)-H(15A)	0.9900
C(15)-H(15B)	0.9900
C(16)-C(17)	1.519(8)
C(16)-H(16A)	0.9900
C(16)-H(16B)	0.9900
C(17)-C(22)	1.362(7)
C(17)-C(18)	1.404(8)
C(18)-C(19)	1.379(8)
C(18)-H(18)	0.9500
C(19)-C(20)	1.397(8)
C(19)-H(19)	0.9500
C(20)-C(21)	1.413(9)
C(20)-H(20)	0.9500
C(21)-C(22)	1.385(8)
C(21)-H(21)	0.9500
C(22)-H(22)	0.9500
C(23)-C(24)	1.502(7)
C(23)-C(28)	1.531(7)
C(23)-H(23)	1.0000
C(24)-C(25)	1.531(8)
C(24)-H(24A)	0.9900
C(24)-H(24B)	0.9900
C(25)-C(26)	1.524(7)
C(25)-H(25A)	0.9900

C(25)-H(25B)	0.9900
C(26)-C(27)	1.500(8)
C(26)-H(26A)	0.9900
C(26)-H(26B)	0.9900
C(27)-C(28)	1.527(8)
C(27)-H(27A)	0.9900
C(27)-H(27B)	0.9900
C(28)-H(28A)	0.9900
C(28)-H(28B)	0.9900
B(1)-H(1A)	0.9800
B(1)-H(1B)	0.9800
B(1)-H(1C)	0.9800
B(2)-H(2A)	0.9800
B(2)-H(2B)	0.9800
B(2)-H(2C)	0.9800
C(1)-P(1)-C(14)	107.1(3)
C(1)-P(1)-C(8)	102.5(3)
C(14)-P(1)-C(8)	105.1(3)
C(1)-P(1)-B(1)	114.8(3)
C(14)-P(1)-B(1)	110.9(3)
C(8)-P(1)-B(1)	115.6(4)
C(15)-P(2)-C(16)	104.6(3)
C(15)-P(2)-C(23)	110.6(3)
C(16)-P(2)-C(23)	101.8(3)
C(15)-P(2)-B(2)	111.3(3)
C(16)-P(2)-B(2)	114.2(3)
C(23)-P(2)-B(2)	113.6(3)
C(2)-C(1)-P(1)	117.5(5)
C(2)-C(1)-H(1D)	107.9
P(1)-C(1)-H(1D)	107.9
C(2)-C(1)-H(1E)	107.9
P(1)-C(1)-H(1E)	107.9
H(1D)-C(1)-H(1E)	107.2

C(3)-C(2)-C(7)	117.4(7)
C(3)-C(2)-C(1)	124.1(7)
C(7)-C(2)-C(1)	118.5(7)
C(2)-C(3)-C(4)	121.5(7)
C(2)-C(3)-H(3)	119.2
C(4)-C(3)-H(3)	119.2
C(5)-C(4)-C(3)	119.1(7)
C(5)-C(4)-H(4)	120.5
C(3)-C(4)-H(4)	120.5
C(4)-C(5)-C(6)	119.2(7)
C(4)-C(5)-H(5)	120.4
C(6)-C(5)-H(5)	120.4
C(7)-C(6)-C(5)	120.4(7)
C(7)-C(6)-H(6)	119.8
C(5)-C(6)-H(6)	119.8
C(6)-C(7)-C(2)	122.3(7)
C(6)-C(7)-H(7)	118.8
C(2)-C(7)-H(7)	118.8
C(13)-C(8)-C(9)	112.4(6)
C(13)-C(8)-P(1)	109.6(5)
C(9)-C(8)-P(1)	111.2(4)
C(13)-C(8)-H(8)	107.8
C(9)-C(8)-H(8)	107.8
P(1)-C(8)-H(8)	107.8
C(8)-C(9)-C(10)	109.4(5)
C(8)-C(9)-H(9A)	109.8
C(10)-C(9)-H(9A)	109.8
C(8)-C(9)-H(9B)	109.8
C(10)-C(9)-H(9B)	109.8
H(9A)-C(9)-H(9B)	108.2
C(11)-C(10)-C(9)	110.6(6)
C(11)-C(10)-H(10A)	109.5
C(9)-C(10)-H(10A)	109.5
C(11)-C(10)-H(10B)	109.5

C(9)-C(10)-H(10B)	109.5
H(10A)-C(10)-H(10B)	108.1
C(10)-C(11)-C(12)	111.8(6)
C(10)-C(11)-H(11A)	109.3
C(12)-C(11)-H(11A)	109.3
C(10)-C(11)-H(11B)	109.3
C(12)-C(11)-H(11B)	109.3
H(11A)-C(11)-H(11B)	107.9
C(11)-C(12)-C(13)	110.3(5)
C(11)-C(12)-H(12A)	109.6
C(13)-C(12)-H(12A)	109.6
C(11)-C(12)-H(12B)	109.6
C(13)-C(12)-H(12B)	109.6
H(12A)-C(12)-H(12B)	108.1
C(8)-C(13)-C(12)	108.4(6)
C(8)-C(13)-H(13A)	110.0
C(12)-C(13)-H(13A)	110.0
C(8)-C(13)-H(13B)	110.0
C(12)-C(13)-H(13B)	110.0
H(13A)-C(13)-H(13B)	108.4
C(15)-C(14)-P(1)	117.1(4)
C(15)-C(14)-H(14A)	108.0
P(1)-C(14)-H(14A)	108.0
C(15)-C(14)-H(14B)	108.0
P(1)-C(14)-H(14B)	108.0
H(14A)-C(14)-H(14B)	107.3
C(14)-C(15)-P(2)	113.1(4)
C(14)-C(15)-H(15A)	109.0
P(2)-C(15)-H(15A)	109.0
C(14)-C(15)-H(15B)	109.0
P(2)-C(15)-H(15B)	109.0
H(15A)-C(15)-H(15B)	107.8
C(17)-C(16)-P(2)	113.1(5)
C(17)-C(16)-H(16A)	109.0

P(2)-C(16)-H(16A)	109.0
C(17)-C(16)-H(16B)	109.0
P(2)-C(16)-H(16B)	109.0
H(16A)-C(16)-H(16B)	107.8
C(22)-C(17)-C(18)	119.7(7)
C(22)-C(17)-C(16)	120.6(6)
C(18)-C(17)-C(16)	119.7(6)
C(19)-C(18)-C(17)	120.0(6)
C(19)-C(18)-H(18)	120.0
C(17)-C(18)-H(18)	120.0
C(18)-C(19)-C(20)	121.7(7)
C(18)-C(19)-H(19)	119.1
C(20)-C(19)-H(19)	119.1
C(19)-C(20)-C(21)	116.5(7)
C(19)-C(20)-H(20)	121.7
C(21)-C(20)-H(20)	121.7
C(22)-C(21)-C(20)	121.8(7)
C(22)-C(21)-H(21)	119.1
C(20)-C(21)-H(21)	119.1
C(17)-C(22)-C(21)	120.2(6)
C(17)-C(22)-H(22)	119.9
C(21)-C(22)-H(22)	119.9
C(24)-C(23)-C(28)	110.7(5)
C(24)-C(23)-P(2)	111.2(4)
C(28)-C(23)-P(2)	112.4(4)
C(24)-C(23)-H(23)	107.4
C(28)-C(23)-H(23)	107.4
P(2)-C(23)-H(23)	107.4
C(23)-C(24)-C(25)	109.1(5)
C(23)-C(24)-H(24A)	109.9
C(25)-C(24)-H(24A)	109.9
C(23)-C(24)-H(24B)	109.9
C(25)-C(24)-H(24B)	109.9
H(24A)-C(24)-H(24B)	108.3

C(26)-C(25)-C(24)	112.1(5)
C(26)-C(25)-H(25A)	109.2
C(24)-C(25)-H(25A)	109.2
C(26)-C(25)-H(25B)	109.2
C(24)-C(25)-H(25B)	109.2
H(25A)-C(25)-H(25B)	107.9
C(27)-C(26)-C(25)	110.8(6)
C(27)-C(26)-H(26A)	109.5
C(25)-C(26)-H(26A)	109.5
C(27)-C(26)-H(26B)	109.5
C(25)-C(26)-H(26B)	109.5
H(26A)-C(26)-H(26B)	108.1
C(26)-C(27)-C(28)	112.7(5)
C(26)-C(27)-H(27A)	109.1
C(28)-C(27)-H(27A)	109.1
C(26)-C(27)-H(27B)	109.1
C(28)-C(27)-H(27B)	109.1
H(27A)-C(27)-H(27B)	107.8
C(27)-C(28)-C(23)	110.2(5)
C(27)-C(28)-H(28A)	109.6
C(23)-C(28)-H(28A)	109.6
C(27)-C(28)-H(28B)	109.6
C(23)-C(28)-H(28B)	109.6
H(28A)-C(28)-H(28B)	108.1
P(1)-B(1)-H(1A)	109.5
P(1)-B(1)-H(1B)	109.5
H(1A)-B(1)-H(1B)	109.5
P(1)-B(1)-H(1C)	109.5
H(1A)-B(1)-H(1C)	109.5
H(1B)-B(1)-H(1C)	109.5
P(2)-B(2)-H(2A)	109.5
P(2)-B(2)-H(2B)	109.5
H(2A)-B(2)-H(2B)	109.5
P(2)-B(2)-H(2C)	109.5

H(2A)-B(2)-H(2C) 109.5

H(2B)-B(2)-H(2C) 109.5

Symmetry transformations used to generate equivalent atoms:

Table 4. Anisotropic displacement parameters ($\text{\AA}^2 \times 10^3$) for bc26. The anisotropic displacement factor exponent takes the form: $-2\pi^2 [h^2 a^{*2} U^{11} + \dots + 2 h k a^* b^* U^{12}]$

	U ¹¹	U ²²	U ³³	U ²³	U ¹³	U ¹²
P(1)	38(1)	58(1)	69(2)	3(1)	12(1)	1(1)
P(2)	36(1)	58(1)	66(2)	-1(1)	12(1)	3(1)
C(1)	41(4)	56(5)	92(7)	8(5)	34(5)	15(4)
C(2)	47(4)	47(5)	42(5)	8(4)	19(4)	7(4)
C(3)	35(4)	59(5)	80(7)	19(5)	14(4)	-11(4)
C(4)	51(5)	70(6)	58(6)	7(5)	19(4)	6(4)
C(5)	57(4)	62(6)	57(6)	6(5)	16(4)	3(4)
C(6)	47(4)	78(6)	64(7)	-4(5)	24(4)	-17(4)
C(7)	43(4)	61(5)	67(7)	-6(5)	10(5)	-2(4)
C(8)	44(4)	54(5)	58(6)	-11(4)	11(4)	-4(4)
C(9)	55(5)	61(5)	59(6)	3(5)	15(4)	13(4)
C(10)	64(5)	58(5)	62(6)	7(5)	22(5)	19(4)
C(11)	42(4)	88(6)	53(6)	1(5)	5(4)	13(4)
C(12)	50(4)	86(6)	65(6)	-12(5)	10(4)	24(4)
C(13)	30(4)	84(6)	69(6)	-1(5)	-1(4)	-6(4)
C(14)	31(3)	43(4)	51(5)	2(4)	10(3)	-5(3)
C(15)	35(4)	46(4)	64(6)	0(4)	11(4)	1(4)
C(16)	37(4)	50(5)	46(5)	-8(4)	1(3)	-2(3)
C(17)	39(4)	61(5)	53(6)	0(4)	11(4)	5(4)
C(18)	38(4)	62(5)	59(6)	-13(5)	12(4)	5(4)
C(19)	55(5)	51(5)	98(8)	-20(5)	33(5)	3(4)
C(20)	61(5)	78(6)	74(7)	-14(5)	22(5)	16(5)
C(21)	43(4)	56(5)	67(6)	15(5)	0(4)	0(4)
C(22)	43(4)	60(5)	46(6)	9(5)	18(4)	6(4)
C(23)	34(3)	58(5)	46(5)	-8(4)	7(3)	3(3)
C(24)	33(4)	79(6)	57(6)	0(5)	4(4)	-8(4)
C(25)	37(4)	64(5)	61(6)	7(5)	5(4)	5(4)
C(26)	57(5)	69(6)	63(6)	-3(5)	20(5)	1(4)
C(27)	34(4)	78(6)	68(6)	1(5)	16(4)	-2(4)

C(28)	33(3)	52(5)	59(5)	-3(5)	9(3)	-5(4)
B(1)	46(5)	63(7)	91(8)	-7(6)	14(5)	-6(5)
B(2)	58(5)	56(6)	68(7)	22(6)	32(5)	27(5)

Table 5. Hydrogen coordinates ($\times 10^4$) and isotropic displacement parameters ($\text{\AA}^2 \times 10^{-3}$) for bc26.

	x	y	z	U(eq)
H(1D)	12039	150	5910	72
H(1E)	11387	-692	5826	72
H(3)	7233	-693	4186	70
H(4)	6075	-541	2220	70
H(5)	8138	173	1312	70
H(6)	11385	673	2350	74
H(7)	12468	513	4258	70
H(8)	11602	714	7667	63
H(9A)	8545	186	8821	70
H(9B)	8422	975	8244	70
H(10A)	11716	1322	9491	72
H(10B)	10105	1055	10211	72
H(11A)	11805	-87	10517	74
H(11B)	13597	534	10902	74
H(12A)	14800	-393	9810	82
H(12B)	14726	392	9226	82
H(13A)	13053	-477	7828	76
H(13B)	11427	-720	8557	76
H(14A)	6651	672	5111	50
H(14B)	6175	834	6293	50
H(15A)	9582	1482	5506	58
H(15B)	9358	1600	6753	58
H(16A)	9657	3105	5861	55
H(16B)	7475	3534	5834	55
H(18)	5891	3390	7529	63
H(19)	6765	3433	9465	79
H(20)	10313	3205	10528	84
H(21)	12869	2831	9548	70

H(22)	11989	2801	7608	58
H(23)	5945	2963	3827	56
H(24A)	3273	2052	3534	69
H(24B)	5014	1450	3409	69
H(25A)	3105	1857	1605	66
H(25B)	3756	2686	1947	66
H(26A)	6680	1559	1668	75
H(26B)	6018	2258	873	75
H(27A)	7820	3036	2266	72
H(27B)	9452	2398	2150	72
H(28A)	9615	2650	4069	58
H(28B)	8957	1816	3759	58
H(1A)	6404	-754	7225	101
H(1B)	7967	-1289	6776	101
H(1C)	5997	-900	5911	101
H(2A)	3302	1751	5505	87
H(2B)	3240	2611	5729	87
H(2C)	4403	2073	6719	87

APPENDIX C

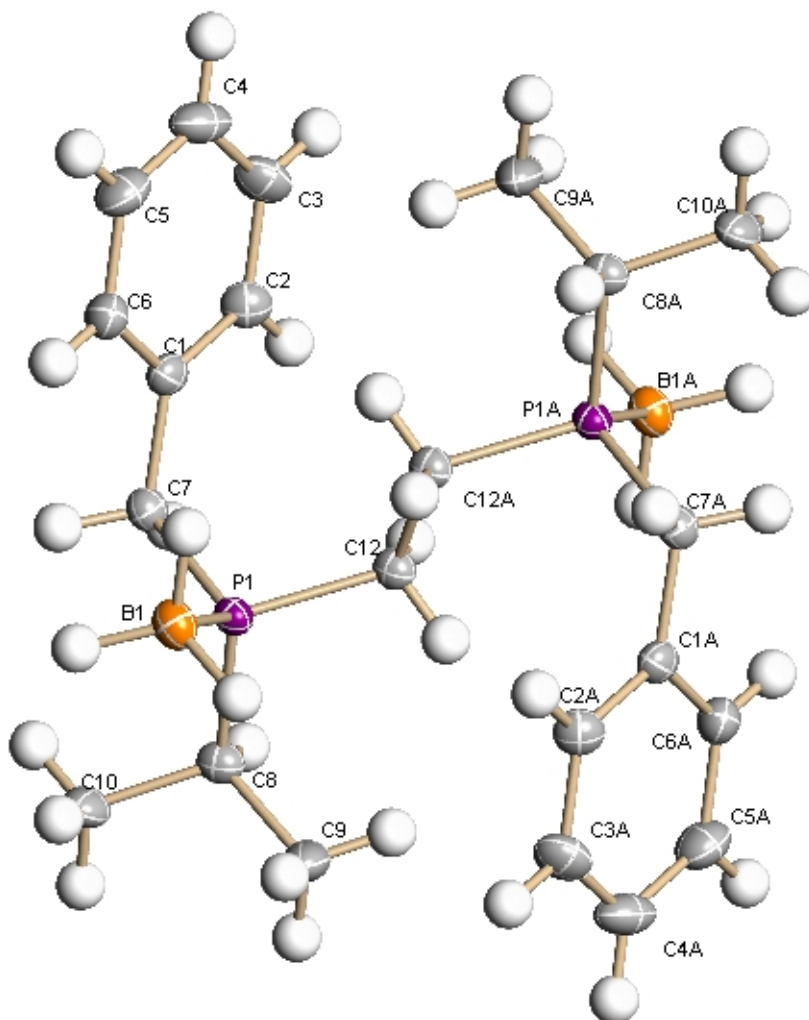
CRYSTAL STRUCTURE OF (*R,R*)-1,2-BIS(BORANATO(*I*-
PROPYL)BENZYLPHOSPHINO)ETHANE

Table 1. Crystal data and structure refinement for bc25a.

Identification code	bc25a	
Empirical formula	C ₂₂ H ₃₈ B ₂ P ₂	
Formula weight	386.08	
Temperature	110(2) K	
Wavelength	1.54178 Å	
Crystal system	Monoclinic	
Space group	P2(1)/c	
Unit cell dimensions	a = 10.658(3) Å	∠ = 90°.
	b = 18.732(6) Å	∠ = 106.05(2)°.
	c = 6.180(2) Å	∠ = 90°.
Volume	1185.6(7) Å ³	
Z	2	
Density (calculated)	1.082 Mg/m ³	
Absorption coefficient	1.661 mm ⁻¹	
F(000)	420	
Crystal size	0.20 x 0.02 x 0.02 mm ³	
Theta range for data collection	4.72 to 59.95°.	
Index ranges	-11 ≤ h ≤ 11, -21 ≤ k ≤ 20, -6 ≤ l ≤ 6	
Reflections collected	10409	
Independent reflections	1624 [R(int) = 0.0605]	
Completeness to theta = 59.95°	93.0 %	
Absorption correction	Semi-empirical from equivalents	
Max. and min. transmission	0.9675 and 0.7324	
Refinement method	Full-matrix least-squares on F ²	
Data / restraints / parameters	1624 / 0 / 131	
Goodness-of-fit on F ²	1.006	
Final R indices [I > 2σ(I)]	R1 = 0.0354, wR2 = 0.0949	
R indices (all data)	R1 = 0.0412, wR2 = 0.0979	
Largest diff. peak and hole	0.303 and -0.295 e.Å ⁻³	

Table 2. Atomic coordinates ($\times 10^4$) and equivalent isotropic displacement parameters ($\text{\AA}^2 \times 10^3$) for bc25a. $U(\text{eq})$ is defined as one third of the trace of the orthogonalized U^{ij} tensor.

	x	y	z	$U(\text{eq})$
P(1)	3784(1)	5988(1)	-206(1)	18(1)
C(1)	6241(1)	6610(1)	98(2)	22(1)
C(2)	7031(2)	6341(1)	-1168(3)	27(1)
C(3)	8370(2)	6283(1)	-230(3)	34(1)
C(4)	8941(2)	6492(1)	1974(3)	37(1)
C(5)	8158(2)	6754(1)	3235(3)	35(1)
C(6)	6828(2)	6810(1)	2317(3)	27(1)
C(7)	4792(2)	6691(1)	-923(2)	22(1)
C(8)	2204(2)	6122(1)	-2297(3)	22(1)
C(9)	1266(2)	5506(1)	-2319(3)	35(1)
C(10)	1603(2)	6833(1)	-1882(3)	29(1)
C(12)	4434(1)	5150(1)	-942(2)	21(1)
B(1)	3689(2)	6020(1)	2846(3)	26(1)

Table 3. Bond lengths [\AA] and angles [$^\circ$] for bc25a.

P(1)-C(12)	1.8240(16)
P(1)-C(7)	1.8295(16)
P(1)-C(8)	1.8350(17)
P(1)-B(1)	1.917(2)
C(1)-C(2)	1.392(2)
C(1)-C(6)	1.392(2)
C(1)-C(7)	1.506(2)
C(2)-C(3)	1.389(3)
C(2)-H(2A)	0.9500
C(3)-C(4)	1.386(3)
C(3)-H(3A)	0.9500
C(4)-C(5)	1.380(2)
C(4)-H(4A)	0.9500
C(5)-C(6)	1.377(2)
C(5)-H(5A)	0.9500
C(6)-H(6A)	0.9500
C(7)-H(7A)	0.9900
C(7)-H(7B)	0.9900
C(8)-C(9)	1.523(2)
C(8)-C(10)	1.529(2)
C(8)-H(8A)	1.0000
C(9)-H(9A)	0.9800
C(9)-H(9B)	0.9800
C(9)-H(9C)	0.9800
C(10)-H(10A)	0.9800
C(10)-H(10B)	0.9800
C(10)-H(10C)	0.9800
C(12)-C(12)#1	1.533(3)
C(12)-H(12A)	0.9600
C(12)-H(12B)	0.9599
B(1)-H(1B)	1.10(2)
B(1)-H(2B)	1.17(2)

B(1)-H(3B)	1.100(18)
C(12)-P(1)-C(7)	105.66(7)
C(12)-P(1)-C(8)	106.24(7)
C(7)-P(1)-C(8)	102.56(7)
C(12)-P(1)-B(1)	113.55(7)
C(7)-P(1)-B(1)	114.20(8)
C(8)-P(1)-B(1)	113.62(9)
C(2)-C(1)-C(6)	118.32(14)
C(2)-C(1)-C(7)	120.70(14)
C(6)-C(1)-C(7)	120.97(14)
C(3)-C(2)-C(1)	120.38(15)
C(3)-C(2)-H(2A)	119.8
C(1)-C(2)-H(2A)	119.8
C(4)-C(3)-C(2)	120.57(17)
C(4)-C(3)-H(3A)	119.7
C(2)-C(3)-H(3A)	119.7
C(5)-C(4)-C(3)	119.10(16)
C(5)-C(4)-H(4A)	120.4
C(3)-C(4)-H(4A)	120.4
C(6)-C(5)-C(4)	120.56(16)
C(6)-C(5)-H(5A)	119.7
C(4)-C(5)-H(5A)	119.7
C(5)-C(6)-C(1)	121.06(16)
C(5)-C(6)-H(6A)	119.5
C(1)-C(6)-H(6A)	119.5
C(1)-C(7)-P(1)	115.40(10)
C(1)-C(7)-H(7A)	108.4
P(1)-C(7)-H(7A)	108.4
C(1)-C(7)-H(7B)	108.4
P(1)-C(7)-H(7B)	108.4
H(7A)-C(7)-H(7B)	107.5
C(9)-C(8)-C(10)	110.88(13)
C(9)-C(8)-P(1)	112.05(11)

C(10)-C(8)-P(1)	110.23(10)
C(9)-C(8)-H(8A)	107.8
C(10)-C(8)-H(8A)	107.8
P(1)-C(8)-H(8A)	107.8
C(8)-C(9)-H(9A)	109.5
C(8)-C(9)-H(9B)	109.5
H(9A)-C(9)-H(9B)	109.5
C(8)-C(9)-H(9C)	109.5
H(9A)-C(9)-H(9C)	109.5
H(9B)-C(9)-H(9C)	109.5
C(8)-C(10)-H(10A)	109.5
C(8)-C(10)-H(10B)	109.5
H(10A)-C(10)-H(10B)	109.5
C(8)-C(10)-H(10C)	109.5
H(10A)-C(10)-H(10C)	109.5
H(10B)-C(10)-H(10C)	109.5
C(12)#1-C(12)-P(1)	113.50(13)
C(12)#1-C(12)-H(12A)	109.3
P(1)-C(12)-H(12A)	109.1
C(12)#1-C(12)-H(12B)	108.3
P(1)-C(12)-H(12B)	108.7
H(12A)-C(12)-H(12B)	107.8
P(1)-B(1)-H(1B)	106.2(10)
P(1)-B(1)-H(2B)	106.0(10)
H(1B)-B(1)-H(2B)	111.7(13)
P(1)-B(1)-H(3B)	106.1(9)
H(1B)-B(1)-H(3B)	110.1(13)
H(2B)-B(1)-H(3B)	115.9(14)

Symmetry transformations used to generate equivalent atoms:

#1 -x+1,-y+1,-z

Table 4. Anisotropic displacement parameters ($\text{\AA}^2 \times 10^3$) for bc25a. The anisotropic displacement factor exponent takes the form: $-2\pi^2 [h^2 a^{*2} U^{11} + \dots + 2 h k a^* b^* U^{12}]$

	U^{11}	U^{22}	U^{33}	U^{23}	U^{13}	U^{12}
P(1)	18(1)	20(1)	17(1)	-1(1)	5(1)	2(1)
C(1)	22(1)	19(1)	27(1)	2(1)	8(1)	-2(1)
C(2)	27(1)	31(1)	25(1)	3(1)	10(1)	-2(1)
C(3)	26(1)	41(1)	39(1)	4(1)	17(1)	3(1)
C(4)	21(1)	39(1)	47(1)	11(1)	4(1)	-3(1)
C(5)	31(1)	36(1)	32(1)	-2(1)	1(1)	-7(1)
C(6)	27(1)	25(1)	29(1)	-4(1)	8(1)	-1(1)
C(7)	23(1)	21(1)	23(1)	2(1)	6(1)	2(1)
C(8)	21(1)	29(1)	18(1)	0(1)	7(1)	1(1)
C(9)	21(1)	29(1)	48(1)	-5(1)	0(1)	-1(1)
C(10)	20(1)	27(1)	37(1)	3(1)	2(1)	4(1)
C(12)	21(1)	24(1)	18(1)	-1(1)	6(1)	1(1)
B(1)	30(1)	27(1)	21(1)	0(1)	9(1)	5(1)

Table 5. Hydrogen coordinates ($\times 10^4$) and isotropic displacement parameters ($\text{\AA}^2 \times 10^{-3}$) for bc25a.

	x	y	z	U(eq)
H(2A)	6651	6197	-2682	33
H(3A)	8900	6097	-1107	40
H(4A)	9858	6456	2608	44
H(5A)	8539	6897	4749	42
H(6A)	6302	6988	3213	32
H(7A)	4616	6707	-2581	27
H(7B)	4518	7155	-436	27
H(8A)	2363	6145	-3816	27
H(9A)	439	5596	-3464	52
H(9B)	1105	5466	-837	52
H(9C)	1649	5061	-2670	52
H(10A)	761	6898	-3008	44
H(10B)	2191	7224	-2000	44
H(10C)	1474	6832	-373	44
H(12A)	4720	5220	-2270	25
H(12B)	3746	4802	-1289	25
H(1B)	4690(20)	5942(9)	3910(30)	48(6)
H(2B)	3000(20)	5548(11)	3030(30)	58(6)
H(3B)	3346(18)	6560(10)	3100(30)	45(5)

—

VITA

Name: Richard P. Sanchez, Jr.

Address: Chemistry Department
c/o Dr. Brian Connell
Texas A&M University
College Station, TX 77843-3255

Email Address: rsanchezjr7@gmail.com

Education: B.A., Science, Texas A&M University Kingsville, 2002
M.S., Chemistry, Texas A&M University Kingsville, 2005
M.S., Chemistry, Texas A&M University, 2009